Disruption of the IS6-AID Linker Affects Voltage-gated Calcium Channel Inactivation and Facilitation

Felix Findeisen and Daniel L. Minor Jr.

Cardiovascular Research Institute, Department of Biochemistry and Biophysics, and Department of Cellular and Molecular Pharmacology, California Institute for Quantitative Biosciences, University of California, San Francisco, San Francisco, CA 94158

Two processes dominate voltage-gated calcium channel (Ca_V) inactivation: voltage-dependent inactivation (VDI) and calcium-dependent inactivation (CDI). The $Ca_V\beta$/$Ca_V\alpha_1$-I-II loop and Ca^{2+}/calmodulin (CaM)/$Ca_V\alpha_1$–C-terminal tail complexes have been shown to modulate each, respectively. Nevertheless, how each complex couples to the pore and whether each affects inactivation independently have remained unresolved. Here, we demonstrate that the IS6–α-interaction domain (AID) linker provides a rigid connection between the pore and $Ca_V\beta$/I-II loop complex by showing that IS6-AID linker polyglycine mutations accelerate $Ca_V1.2$ (L-type) and $Ca_V2.1$ (P/Q-type) VDI. Remarkably, mutations that either break the rigid IS6-AID linker connection or disrupt $Ca_V\beta$/I-II association sharply decelerate CDI and reduce a second Ca^{2+}/CaM/$Ca_V\alpha_1$–C-terminal–mediated process known as calcium-dependent facilitation. Collectively, the data strongly suggest that components traditionally associated solely with VDI, $Ca_V\beta$ and the IS6-AID linker, are essential for calcium-dependent modulation, and that both $Ca_V\beta$-dependent and CaM-dependent components couple to the pore by a common mechanism requiring $Ca_V\beta$ and an intact IS6-AID linker.

INTRODUCTION

Voltage-gated calcium channels (Ca_Vs) serve as a major source of calcium influx in excitable cells (Hille, 2001). Calcium ions have a unique biological role in that they act as both charge carriers and as chemical messengers (Clapham, 2007). Thus, Ca_V activity provides a vital link between membrane potential charges and stimulation of calcium-driven intracellular signaling cascades that directly affect processes such as excitation–contraction coupling, neurotransmitter release, and gene regulation (Catterall, 2000). High voltage–activated channels consist of four essential components (Van Petegem and Minor, 2006): a pore-forming $Ca_V\alpha_1$ subunit from either Ca_V1 or Ca_V2 isoforms (Catterall, 2000), a cytoplasmic $Ca_V\beta$ subunit (Dolphin, 2003), the transmembrane $Ca_V\alpha_2\delta$ subunit (Davies et al., 2007), and calmodulin (CaM) (Pitt, 2007). Two intracellular components of the complex, $Ca_V\beta$ and CaM, play central roles in channel modulation processes that affect calcium influx. In particular, both affect channel inactivation, a generalized term for phenomena that limit channel conduction and calcium influx under conditions in which the channel would otherwise remain open.

The two principal Ca_V inactivation processes are voltage-dependent inactivation (VDI) (Stotz et al., 2004; Cens et al., 2006) and calcium-dependent inactivation (CDI) (Cens et al., 2006; Halling et al., 2006). The molecular origins of VDI are complex and have remained imperfectly understood (Stotz et al., 2004). The predominant contributions appear to arise from the $Ca_V\beta$ subunit (Olcese et al., 1994; Stea et al., 1994; De Waard and Campbell, 1995), $Ca_V\alpha_1$ transmembrane segment IS6 (Zhang et al., 1994; Raybaud et al., 2006), and the $Ca_V\alpha_1$ intracellular I-II loop (Herlitze et al., 1997; Sokolov et al., 1999; Stotz et al., 2000; Berrou et al., 2001; Geib et al., 2002), although mutations in other transmembrane segments (Stotz et al., 2000; Berjukow et al., 2001; Shi and Soldatov, 2002; Raybaud et al., 2006, 2007), the cytoplasmic N-terminal domain (Kobrinsky et al., 2005; Kanevsky and Dascal, 2006), the C-terminal EF-hand region (Bernatchez et al., 1998), and the CaM-interaction domain (Liang et al., 2003; Kim et al., 2004; Barrett and Tsien, 2008) have also been shown to affect VDI. The central role of $Ca_V\beta$ in VDI is evident from the diverse VDI rates bestowed upon Ca_V1 and Ca_V2 $Ca_V\alpha_1$ subunits through association with particular $Ca_V\beta$ isoforms. $Ca_V\beta_{2a}$ slows VDI considerably (Olcese et al., 1994; Stea et al., 1994; De Waard and Campbell, 1995), a consequence of the anchoring of its N terminus to the membrane by palmitoylation (Chien et al., 1996; Qin et al., 1998). In contrast, $Ca_V\beta_1$, $Ca_V\beta_{2b}$, and $Ca_V\beta_3$, which lack

Correspondence to Daniel L. Minor Jr.: daniel.minor@ucsf.edu

Abbreviations used in this paper: AID, α-interaction domain; CaM, calmodulin; Ca_V, voltage-gated calcium channel; CD, circular dichroism; CDF, calcium-dependent facilitation; CDI, calcium-dependent inactivation; TEV, tobacco etch mosaic virus; TFE, trifluoroethanol; VDI, voltage-dependent inactivation.

© 2009 Findeisen and Minor This article is distributed under the terms of an Attribution–Noncommercial–Share Alike–No Mirror Sites license for the first six months after the publication date (see http://www.jgp.org/misc/terms.shtml). After six months it is available under a Creative Commons License (Attribution–Noncommercial–Share Alike 3.0 Unported license, as described at http://creativecommons.org/licenses/by-nc-sa/3.0/).

The Rockefeller University Press $30.00
J. Gen. Physiol. Vol. 133 No. 3 327–343
www.jgp.org/cgi/doi/10.1085/jgp.200810143

The Journal of General Physiology

Downloaded from http://rupress.org/jgp/article-pdf/133/3/327/1914330/jgp_200810143.pdf by guest on 09 February 2026

the palmitoylation site found in $Ca_V\beta_{2a}$, support fast VDI (Olcese et al., 1994; Stea et al., 1994; De Waard and Campbell, 1995). The discovery that IS6 mutations that drastically reduce $Ca_V1.2$ VDI cause a multisystem disorder involving lethal heart arrhythmias, cognitive abnormalities, and immune deficiencies, known as Timothy syndrome (Splawski et al., 2004, 2005), provides further evidence for the importance of IS6 in channel gating and a compelling example of the physiological relevance of VDI.

Structural studies have revealed that the high affinity $Ca_V\beta$-binding site present on the I-II loop, the α-interaction domain (AID), forms an α-helix that interacts extensively with a deep pocket on $Ca_V\beta$, the α-binding pocket (Chen et al., 2004; Opatowsky et al., 2004; Van Petegem et al., 2004). Although absent from the crystal structures, the 22 residues that bridge the C-terminal cytoplasmic end of the pore-lining IS6 helix and N-terminal end of the AID α-helix, the IS6-AID linker, have been noted to have a high α-helix propensity (Opatowsky et al., 2004; Van Petegem et al., 2004). This observation raises the possibility that the IS6-AID linker forms a continuous helix between IS6 and AID that acts as a rigid rod through which $Ca_V\beta$ affects channel gating (Opatowsky et al., 2004; Van Petegem et al., 2004). Partial support for this idea comes from functional studies of chimeras between the low voltage–activated $Ca_V3.1$, a $Ca_V\alpha_1$ subunit that lacks $Ca_V\beta$ modulation, and the $Ca_V2.2$ I-II loop (Arias et al., 2005). Fusion of the $Ca_V2.2$ I-II loop to the end of $Ca_V3.1$ IS6 endowed the chimeric channel with $Ca_V\beta$-dependent modulation that could be eliminated by hexaglycine mutations in the IS6-AID linker. Nevertheless, a detailed investigation of the role of the IS6-AID linker in the context of channels that are natively modulated by $Ca_V\beta$s has not been reported.

Ca^{2+}/CaM binding to the IQ domain, which is located in the $Ca_V\alpha_1$ subunit cytoplasmic C-terminal tail, drives CDI (Zühlke et al., 1999; Erickson et al., 2003; Halling et al., 2006) as well as calcium-dependent facilitation (CDF), an increase in peak current upon repetitive stimuli (Zühlke et al., 1999; DeMaria et al., 2001; Van Petegem et al., 2005; Lee et al., 2006). The IQ domain is ∼200 residues C terminal to the last transmembrane segment IVS6. Although crystallographic studies have revealed the nature of the Ca^{2+}/CaM-IQ domain interaction (Fallon et al., 2005; Van Petegem et al., 2005), it is not known how the binding of Ca^{2+}/CaM to a site seemingly distant from the transmembrane pore affects gating.

Even though many models have been proposed, it is unclear how VDI and CDI proceed and whether they use separate (Barrett and Tsien, 2008) or common mechanisms (Cens et al., 1999; Kim et al., 2004). Here, we show that both the $Ca_V\beta$ subunit and the integrity of the IS6-AID linker affect VDI, CDI, and CDF profoundly, and that an intact IS6-AID linker is required for both the $Ca_V\beta$ and Ca^{2+}/CaM-IQ domain cytoplasmic elements to modulate the activity of the transmembrane pore. These results provide strong evidence for a model in which VDI, CDI, and CDF act through mediation of the protein–protein complex formed by $Ca_V\beta$ and the IS6-AID linker.

MATERIALS AND METHODS

Molecular Biology

Constructs for electrophysiology consisted of human $Ca_V1.2$ (α_1C77; GenBank accession no. CAA84346) in pcDNA3.1 (Invitrogen), rabbit $Ca_V2.1$ (GenBank accession no. X57477) in pGEMHE, rabbit $Ca_V\beta_1$ (GenBank accession no. M25514) in pSP65, rat $Ca_V\beta_{2a}$ (GenBank accession no. NP_446303) in pGEMHE, rabbit $Ca_V\beta_{2b}$ (GenBank accession no. X64298) in pSPORT1 (Promega), and rabbit $Ca_V\alpha_2\delta$-1 (GenBank accession no. NM_001082276) in pcDNA3.1. ss$Ca_V\beta_{2a}$ is a double mutant (C3S and C4S) of rat $Ca_V\beta_{2a}$. To facilitate mutagenesis of the I-II loop region of $Ca_V1.2$, a silent HpaI site was added at nucleotide positions 1,114–1,119 to create an excisable fragment framed by the HpaI site and a naturally occurring PpuMI site at nucleotide positions 2,759–2,765. This fragment was excised and ligated into a pGEMHE backbone to serve as a template for mutagenesis. Similarly, for $Ca_V2.1$ I-II loop mutagenesis, a ClaI site from the vector N terminal to the $Ca_V2.1$ coding region and the naturally occurring XhoI site at nucleotide positions 1,395–1,400 framed a fragment that was excised and ligated into a pGEMHE backbone to serve as a cloning cassette. Mutations were introduced in the cloning cassette using QuikChange (Agilent Technologies), and mutated fragments were religated into their parent vector. Each mutant was sequenced in the final vector across either the entire channel coding sequence or the mutated fragment and points of reinsertion only, as appropriate.

Electrophysiological Recordings and Data Analysis

After overnight linearization of the vector (pCDNA3 with XhoI, pGEMHE with NheI, pSPORT1 with NotI, and pSP65 with XbaI), capped mRNA was synthesized with the T7 or SP6 Messenger kit (Applied Biosystems), as appropriate. 50 nl of equimolar $Ca_V\alpha_1$, $Ca_V\beta$, and $Ca_V\alpha_2\delta$-1 mRNA at final concentrations of 33–100 nM were injected into de-folliculated *Xenopus* oocytes prepared as described previously (Van Petegem et al., 2005). Two-electrode voltage clamp experiments were performed 2–5 d after injection using a GeneClamp 500B (MDS Analytical Technologies) amplifier controlled by a 1,200-MHz processor computer (Celeron; Gateway) running CLAMPEX 8.2.0.244 and digitized at 1 kHz with a Digidata 1332A (MDS Analytical Technologies). Immediately before recording, oocytes were injected with 50 nl of 100 mM BAPTA to minimize Ca^{2+}-activated Cl^- current. Recording solutions contained either 40 mM $Ba(OH)_2$ or 40 mM $Ca(NO_3)_2$, 50 mM NaOH, 1 mM KOH, and 10 mM HEPES. Both solutions were adjusted to pH 7.4 using HNO_3. Electrodes were filled with 3M KCl and had resistances of 0.3–2.0 MΩ. Leak currents were subtracted using a P/4 protocol. Currents were analyzed with Clampfit 8.2 (MDS Analytical Technologies). During recordings, oocytes were superfused using a Valvelink 16 controller (Automate Scientific). All results are from at least two independent oocyte batches. G_{max}, $V_{0.5}$, and K_a were calculated by recording a series of 450-ms pulses from −50 to +70 mV from a resting potential of −90 mV and fitting them to the equation: $I = G_{max} * (V_m - V_{rev})/(1 + \exp(V_{0.5} - V_m)/K_a)$, where I is the measured peak current at each V_m, G_{max} is the maximal conductance, V_m is the test potential, V_{rev} is the reversal potential, $V_{0.5}$ is the midpoint of activation, and K_a is the slope factor (Kanevsky and Dascal, 2006). The t_{i300} and t_{i2400}

Downloaded from http://rupress.org/jgp/article-pdf/133/3/327/1914330/jgp_200810143.pdf by guest on 09 February 2026

values were calculated from normalized currents at +20 mV and represent the percentage inactivation after 300 and 2,400 ms, respectively. $Ca_V1.2$ currents recorded with calcium as charge carrier show inactivation resulting from two inactivation processes, VDI and CDI. netCDI was determined by dividing the normalized calcium current by the normalized barium current (Barrett and Tsien, 2008). Inactivation τ values were calculated at a test potential of +20 mV using the formula $I = A_1 \exp(-t/\tau_1) + A_2 \exp(-t/\tau_2) + C$, where I is the recorded current, A is the amplitude of the current component, and C is the residual current at steady state. Isochronal inactivation data were obtained using a protocol modified from Berrou et al. (2001) in which a +20-mV control pulse was followed by a 2-s prepulse to variable potentials and a test pulse to +20 mV. Inactivation in both barium and calcium were measured from the same oocyte and calculated as: $\text{Inactivation}_{(\text{Ba or Ca})} = 1 - (i_{test}/i_{control})$ and $\text{Inactivation}_{(\text{netCDI})} = 1 - (1 - \text{Inactivation}_{(\text{Ca})})/(1 - \text{Inactivation}_{(\text{Ba})})$. CDF was elicited by a train of 40 50-ms pulses to +20 mV at a frequency of 3 Hz and calculated as the ratio of the peak current from the last pulse divided by the first.

Protein Expression and Purification

Wild-type and mutant IS6-AID linker peptides (residues 406–427) expressed as fusion proteins in a pET28 vector, called HMT (Van Petegem et al., 2004), which contains in sequence a hexahistidine tag, maltose-binding protein, and tobacco etch mosaic virus (TEV) protease cleavage site followed by the peptide of interest. HMT fusions were expressed in *Escherichia coli* BL21 (DE3)-pLysS using 2YT media (Teknova) at 37°C and induced at $OD_{600nm} = 0.6$, with 0.4 mM IPTG for 4 h. Cells were harvested by centrifugation at 6,000 *g* for 20 min at 4°C. Pellets were stored frozen at −20°C until further use. Thawed cells were lysed by sonication in 250 mM KCl and 10 mM KH_2PO_4/K_2HPO_4, pH 7.3 (Buffer A). After centrifugation at 15,000 *g* at 4°C for 30 min, the soluble fraction was loaded on a nickel-charged Poros20MC column (Applied Biosystems), washed in Buffer A, and eluted using step elution of Buffer A plus 500 mM imidazole, pH 8.0. After overnight cleavage with TEV protease (Kapust et al., 2001) at room temperature, the peptides retained an N-terminal tripeptide sequence of Gly-His-Met derived from the TEV cleavage site and a C-terminal tripeptide sequence of Gly-Gly-Trp to allow determination of the peptide concentration. Pure peptide was eluted in Buffer A as the flow-through from an amylose column (New England Biolabs, Inc.) and a Poros20MC column connected in sequence. Aggregated peptide was separated from soluble material using a Superdex75 HR10/30 gel filtration column (GE Healthcare) in Buffer A. The peptide was concentrated using a Vivaspin 15R with a molecular weight cutoff of 2 kD (Vivascience) to 0.05 mM as determined by absorbance (Edelhoch, 1967).

Circular Dichroism (CD)

CD spectra were measured in a 2-mm path-length quartz cuvette (Hellma), 50 mM KCl, and 10 mM KH_2PO_4/K_2HPO_4, pH 7.3, and varying trifluoroethanol (TFE) concentrations using an Aviv Model 215 spectropolarimeter (Aviv Biomedical) equipped with a peltier temperature controller. Wavelength scans from 320 to 190 nm were taken at 4°C. Each point was determined in triplicate from the same sample and subtracted by the average of a triplicate buffer scan. Each sample was checked for purity by HPLC. Molar ellipticity was calculated as follows: $\theta = 100(\Delta m)/Cnl$, where Δm is the CD signal in millidegrees after buffer subtraction, C is the peptide concentration in millimoles, n is the number of residues in the peptide, and l is the cuvette path length in centimeters. Fraction helix was calculated as $F_{helix} = ([\theta]_{obs} - [\theta]_{coil})/([\theta]_{helix} - [\theta]_{coil})$, where $([\theta]_{helix}$ and $[\theta]_{coil}$ signify the mean residue ellipticity that is +640 for random coil and $-42{,}500*(1-3/n)$ for complete helix, respectively (Rohl et al., 1996).

Online Supplemental Material

Fig. S1 shows the effects of the GGG mutation on $Ca_V1.2$ in the absence of $Ca_V\beta$. Fig. S2 shows the influence of $Ca_V\alpha_2\delta$ on $Ca_V1.2$ $V_{0.5}$. Fig. S3 displays the averaged $V_{0.5}$ values of $Ca_V1.2$ mutations in barium- and calcium-containing buffers. Fig. S4 shows the effect of $Ca_V\beta$ titration on $Ca_V1.2$ and $Ca_V1.2$ GGG G_{max} values. Fig. S5 compares calcium currents for $Ca_V1.2$ 6G, $Ca_V1.2$ GGG/HotA, and wild-type Ca_V 1.2 expressed at similar levels. Table S1 lists the inactivation parameters in calcium-containing buffer for all $Ca_V1.2/Ca_V\beta$ combinations tested. Table S2 presents the current ranges recorded for the channels used in this study. The online supplemental material is available at http://www.jgp.org/cgi/content/full/jgp.200810143/DC1.

RESULTS

Glycine Substitution in the IS6-AID Linker Affects VDI

As noted previously (Opatowsky et al., 2004; Van Petegem et al., 2004), the IS6-AID linker has a high probability to form an α-helical structure (Fig. 1 A). To disrupt the integrity of this putative helix, we mutated three consecutive residues in the middle of the $Ca_V1.2$ IS6-AID linker, residues 415–417, to glycine (denoted as GGG) (Fig. 1 A). Due to the extremely low helix propensity of glycine (O'Neil and DeGrado, 1990; Blaber et al., 1993), the GGG mutation is expected to cause substantial disruption of any helical structure present in the IS6-AID linker, as it should incur an ∼3–kcal mol^{-1} destabilization of the helical conformation. As a control for effects resulting from side chain deletion, we also made a mutant that converts $Ca_V1.2$ residues 415–417 into a triple-alanine sequence, denoted as AAA. Based on the high helix–forming propensity of alanine, this substitution should leave the IS6-AID helix intact.

We used two-electrode voltage clamp recording in *Xenopus* oocytes under conditions in which barium was the charge carrier to examine the consequences of IS6-AID linker mutations in the presence or absence of $Ca_V\beta_{2a}$ modulation. When coexpressed with $Ca_V\beta_{2a}$, GGG channels inactivated ∼7.6-fold faster than wild-type $Ca_V1.2$ channels (τ_1 = 489 ± 130 ms vs. 3,730 ± 670 ms, respectively) and to a sixfold greater extent at 300 ms after activation (t_{i300} = 13.2 ± 2.5% and 2.2 ± 1.3%, respectively) (Fig. 1, B and C, and Table I). In contrast, AAA mutant channels displayed VDI τ and t_{i300} values similar to wild-type $Ca_V1.2$ (τ_1 = 3,290 ± 160 ms; t_{i300} = 1.1 ± 0.6). This result indicates that the functional effects caused by the GGG substitution do not result from the loss of key side chain interactions, but rather from the likely loss of structure in the IS6-AID linker. Further disruption of the IS6-AID linker by a hexa-glycine mutant ($Ca_V1.2$ 6G) (Fig. 1 A) resulted in channels having VDI properties that were indistinguishable from $Ca_V1.2$ GGG channels (τ_1 = 485 ± 155 ms; t_{i300} = 13.0 ± 5.6%) (Fig. 1, B and C, and Table I). In contrast, the corresponding hexa-alanine mutation ($Ca_V1.2$ 6A) had properties similar to wild-type channels (Table I). Thus, additional disruption of the

Downloaded from http://rupress.org/jgp/article-pdf/133/3/327/1914330/jgp_200810143.pdf by guest on 09 February 2026

IS6-AID linker had no further functional consequences on VDI beyond what was observed for the GGG mutant.

$Ca_V1.2$ GGG expressed without $Ca_V\beta_{2a}$ shows VDI that is 1.8-fold faster than $Ca_V1.2$ expressed without $Ca_V\beta_{2a}$ (Table I and Fig. S1), a difference that could indicate that the GGG mutation is able to affect the $Ca_V\alpha_1$ subunit VDI response in the absence of $Ca_V\beta$ modulation. *Xenopus* oocytes are known to express $Ca_V\beta_3$ (Tareilus et al., 1997), a subunit that accelerates VDI and whose presence could confound interpretation of experiments in which $Ca_V\alpha_1$ subunits are expressed in the absence of $Ca_V\beta$ coinjection. To get a cleaner assessment regarding whether the GGG mutation affects $Ca_V\alpha_1$ subunit VDI properties, we examined the effect of the GGG mutant in the context of $Ca_V\alpha_1$ subunits that bear a triple mutant in the $Ca_V\beta$ high affinity binding site, denoted as HotA, which renders the channels incapable of binding $Ca_V\beta$ (Van Petegem et al., 2008). The inactivation properties $Ca_V1.2$ HotA and $Ca_V1.2$ GGG/HotA (Fig. S1) are indistinguishable (τ = 601 ± 211 ms and 607 ± 277 ms, respectively; P = 0.99). Further, the VDI τ values are similar to $Ca_V1.2$ alone. (τ_1 = 455 ± 99 ms) (Fig. 1, B and C, and Table I). These results indicate that the VDI properties of the $Ca_V1.2$ α_1 subunit in the absence of $Ca_V\beta$ modulation are unaffected by the GGG mutation. The VDI τ values and extent of inactivation for the HotA channels were not significantly different from GGG and 6G channels coexpressed with $Ca_V\beta_{2a}$ (Table I) (one-way ANOVA for VDI τ values, P = 0.45; t_{i300}, P = 0.28). Thus, the effects of the glycine mutants on VDI appear to arise from the loss of the influence of $Ca_V\beta_{2a}$ modulation and indicate that the intact IS6-AID linker is required for functional modulation of VDI by $Ca_V\beta_{2a}$.

In addition to the faster τ values and increased extent of inactivation, $Ca_V1.2$ GGG channels lacked the characteristic hyperpolarizing shift in the G-V relationship caused by $Ca_V\beta_{2a}$ coexpression (Perez-Reyes et al., 1992; Neely et al., 1993; Yamaguchi et al., 2000) (Fig. 1 D, Figs. S2 and S3 A, and Table II) and were not significantly different from channels expressed in the absence of $Ca_V\beta_{2a}$ or from $Ca_V1.2$ HotA. In contrast, AAA channels had biophysical properties that

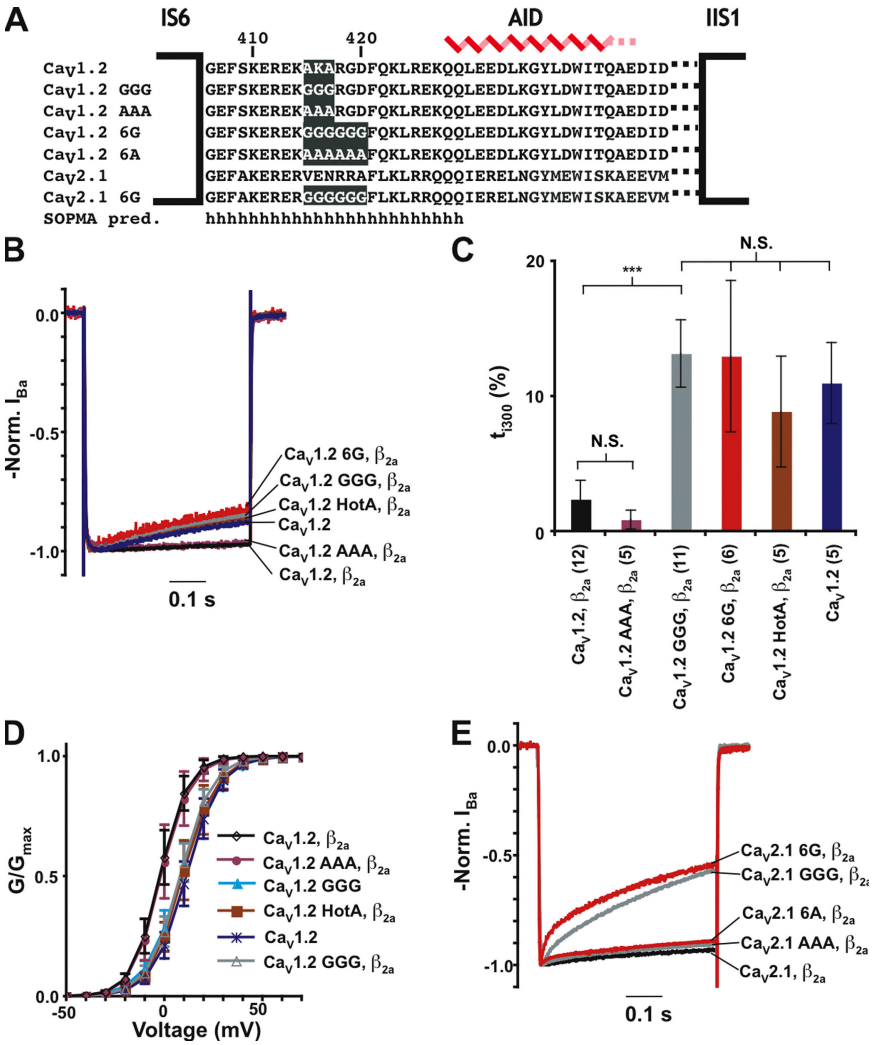

Figure 1. Glycine substitution in the IS6-AID linker affects VDI. (A) Amino acid sequence of wild-type and mutant IS6-AID linker sequences from $Ca_V1.2$ and $Ca_V2.1$. SOPMA secondary structure prediction is indicated (Geourjon and Deleage, 1995). (B) Disruption of the IS6-AID linker accelerates $Ca_V1.2$ VDI. Representative normalized I_{Ba} traces at a test potential of +20 mV for the combination of the indicated $Ca_V1.2$ subunits and $Ca_V\beta_{2a}$. (C) t_{i300} values for data from B. Results of unpaired *t* tests or one-way ANOVA, as appropriate, are indicated as follows: N.S., P > 0.05, not significant; ***, P < 0.001. (D) G-V relationships in barium for the indicated combinations of $Ca_V1.2$ subunits and $Ca_V\beta_{2a}$. (E) Disruption of the IS6-AID linker accelerates $Ca_V2.1$ VDI. Representative normalized I_{Ba} traces of $Ca_V2.1$ wild-type and $Ca_V2.1$ GGG. Data in all figures are represented as mean ± SD.

Downloaded from http://rupress.org/jgp/article-pdf/133/3/327/1914330/jgp_200810143.pdf by guest on 09 February 2026

were indistinguishable from wild-type $Ca_V1.2$ (Fig. 1 D, Fig. S3 A, and Table II).

Even though the GGG mutant does not affect any residues that are important for the AID-$Ca_V\beta$ high affinity interaction (Van Petegem et al., 2008), it was important to test whether the loss of modulation in the GGG background arose from an unexpected effect on $Ca_V\beta_{2a}$ association with the pore-forming subunit. $Ca_V\beta_{2a}$ coexpression potently stimulates the total macroscopic current on wild-type $Ca_V1.2$ channels (Perez-Reyes et al., 1992; Neely et al., 1993), an effect that was retained for $Ca_V\beta_{2a}$ coexpression with $Ca_V1.2$ GGG (Fig. S4). Thus, the changes in both VDI and G-V modulation resulting from glycine mutations in the IS6-AID linker must arise from a loss of functional coupling and not from a loss of the physical interaction between $Ca_V\beta_{2a}$ and the $Ca_V\alpha_1$ subunit.

To test if the importance of the IS6-AID linker for VDI generalized to other high voltage–activated Ca_Vs, we made the analogous substitutions in the IS6-AID linker of a Ca_V2 α_1-subunit, $Ca_V2.1$ (Fig. 1 A). Similar to the effects of the triple-glycine substitution in $Ca_V1.2$, coexpression of $Ca_V2.1$ GGG with $Ca_V\beta_{2a}$ results in channels having greatly increased VDI compared with wild type (Fig. 1 E and Table I). The $Ca_V2.1$ GGG mutation caused a new fast inactivation component (τ_2 = 17.8 ± 2.2 ms), increased the extent of the main inactivation component by approximately sixfold relative to wild type (A_1 = 10.0 ± 1.3% vs. A_1 = 59.3 ± 8.6%, respectively), and brought

TABLE I

Ca_V1 and Ca_V2 Inactivation Properties

Construct	t_{i300} (%)	t_{i2400} (%)	A_1 (%)	τ_1 (ms)	A_2 (%)	τ_2 (ms)	*n*
VDI							
$Ca_V1.2$, β_{2a}	2.2 ± 1.3	10.9 ± 2.6	20.9 ± 3.6	3,730 ± 670	—	—	12
$Ca_V1.2$ AAA, β_{2a}	1.1 ± 0.6	11.9 ± 5.2	18.5 ± 7.5	3,290 ± 160	—	—	5
$Ca_V1.2$ 6A, β_{2a}	1.8 ± 0.6	16.1 ± 3.1	16.9 ± 1.6	1,880 ± 160	—	—	5
$Ca_V1.2$, β_1	22.3 ± 1.8	62.4 ± 5.2	73.0 ± 5.7	1,150 ± 80	—	—	5
$Ca_V1.2$, β_{2b}	4.8 ± 1.5	25.2 ± 2.1	44.5 ± 4.9	2,840 ± 630	—	—	8
$Ca_V1.2$, ssβ_{2a}	7.1 ± 2.9	33.5 ± 7.7	43.3 ± 11.3	2,050 ± 510	—	—	6
$Ca_V1.2$	11.0 ± 3.0	ND	22.7 ± 3.9	455 ± 99	—	—	5
$Ca_V1.2$ HotA, β_{2a}	8.9 ± 4.1	ND	23.6 ± 7.2	601 ± 211	—	—	5
$Ca_V1.2$ GGG, β_{2a}	13.2 ± 2.5	ND	30.0 ± 6.6	489 ± 130	—	—	11
$Ca_V1.2$ 6G, β_{2a}	13.0 ± 5.6	ND	34.2 ± 3.4	485 ± 155	—	—	6
$Ca_V1.2$ GGG/HotA, β_{2a}	8.9 ± 5.6	ND	21.7 ± 7.6	607 ± 277	—	—	7
$Ca_V1.2$ GGG	28.1 ± 3.6	ND	41.9 ± 3.8	255 ± 20	—	—	7
$Ca_V1.2$ GGG, β_1	59.6 ± 4.3	ND	79.2 ± 3.7	202 ± 12	—	—	6
$Ca_V1.2$ GGG, β_{2b}	42.8 ± 3.2	ND	66.0 ± 1.7	264 ± 14	—	—	6
$Ca_V1.2$ GGG, ssβ_{2a}	47.7 ± 2.8	ND	72.0 ± 5.6	262 ± 14	—	—	5
$Ca_V2.1$, β_{2a}	6.5 ± 1.2	ND	9.7 ± 1.5	308 ± 80	—	—	10
$Ca_V2.1$ GGG, β_{2a}	36.9 ± 4.1	ND	59.3 ± 8.6	439 ± 42	9.2 ± 1.9	17.8 ± 2.2	6
$Ca_V2.1$ 6G, β_{2a}	39.5 ± 9.8	ND	45.3 ± 8.0	326 ± 31	14.5 ± 4.1	13.0 ± 2.3	7
$Ca_V2.1$ AAA, β_{2a}	8.2 ± 1.2	ND	11.9 ± 1.6	283 ± 53	—	—	7
$Ca_V2.1$ 6A, β_{2a}	9.6 ± 1.5	ND	14.2 ± 2.2	311 ± 79	—	—	7
$Ca_V2.1$, β_1	57.3 ± 4.3	ND	77.1 ± 7.1	340 ± 55	13.7 ± 2.9	43.9 ± 7.3	8
$Ca_V2.1$ GGG, β_1	98.0 ± 5.1	ND	63.3 ± 2.3	10.1 ± 1.2	36.9 ± 4.1	94.1 ± 10.2	7
netCDI							
$Ca_V1.2$, β_{2a}	69.5 ± 2.6	ND	51.1 ± 2.7	20.3 ± 4.2	19.6 ± 2.7	96.8 ± 25.6	9
$Ca_V1.2$ AAA, β_{2a}	72.3 ± 3.4	ND	53.3 ± 5.1	17.8 ± 1.3	20.4 ± 2.9	98.7 ± 25.9	5
$Ca_V1.2$ 6A, β_{2a}	60.5 ± 3.3	ND	40.4 ± 4.0	24.8 ± 1.0	21.8 ± 1.7	118 ± 13	5
$Ca_V1.2$, β_1	75.3 ± 1.7	ND	57.0 ± 2.1	27.0 ± 1.8	23.1 ± 2.4	177 ± 32	5
$Ca_V1.2$, β_{2b}	72.9 ± 1.7	ND	55.9 ± 3.2	25.4 ± 1.3	20.9 ± 1.0	165 ± 22	5
$Ca_V1.2$	36.6 ± 1.3	ND	34.2 ± 4.2	216 ± 55	12.1 ± 2.0	40.7 ± 13.0	6
$Ca_V1.2$ HotA, β_{2a}	35.6 ± 4.2	ND	33.0 ± 4.3	239 ± 42	12.6 ± 1.9	45.3 ± 9.9	5
$Ca_V1.2$ GGG, β_{2a}	43.7 ± 3.6	ND	37.2 ± 2.1	217 ± 16	16.9 ± 4.1	40.9 ± 5.4	8
$Ca_V1.2$ GGG/HotA, β_{2a}	15.6 ± 6.2	ND	20.7 ± 6.1	258 ± 86	—	—	7
$Ca_V1.2$ 6G, β_{2a}	19.8 ± 5.4	ND	25.4 ± 8.9	214 ± 54	—	—	8
$Ca_V1.2$ GGG, β_1	41.9 ± 3.8	ND	57.9 ± 3.9	350 ± 31	9.5 ± 4.1	56.2 ± 8.6	5
$Ca_V1.2$ GGG, β_{2b}	42.2 ± 4.3	ND	50.4 ± 10.3	356 ± 92	18.4 ± 2.0	54.7 ± 10.5	4

Data are expressed as mean values ± SD. τ values were determined at a holding potential of +20 mV (see Materials and methods). t_{i300} and t_{i2400} denote percent inactivation at 300 and 2,400 ms, respectively. ND, a value not determined.

Downloaded from http://rupress.org/jgp/article-pdf/133/3/327/1914330/jgp_200810143.pdf by guest on 09 February 2026

TABLE II

$Ca_V1.2$ and Mutant $Ca_V1.2$ G-V Relationships

	Ba^{2+}		Ca^{2+}	
Construct	$V_{0.5}$ (mV)	K_a	$V_{0.5}$ (mV)	K_a
$Ca_V1.2$, β_{2a}	−2.1 ± 3.1	7.0 ± 0.5	7.8 ± 2.6	9.2 ± 0.8
$Ca_V1.2$ AAA, β_{2a}	−0.7 ± 4.4	6.7 ± 1.2	7.6 ± 2.9	8.7 ± 0.8
$Ca_V1.2$	11.2 ± 3.2	8.2 ± 1.0	21.0 ± 1.7	10.1 ± 0.5
$Ca_V1.2$ HotA, β_{2a}	9.6 ± 4.3	8.1 ± 1.4	20.9 ± 1.4	10.2 ± 0.4
$Ca_V1.2$ GGG, β_{2a}	8.2 ± 2.5	8.0 ± 0.8	16.8 ± 3.2	9.9 ± 0.7
$Ca_V1.2$ 6G, β_{2a}	4.7 ± 2.4	7.7 ± 0.9	18.4 ± 2.0	9.7 ± 0.9
$Ca_V1.2$ GGG	8.8 ± 3.9	8.8 ± 1.0	16.5 ± 3.4	10.7 ± 0.8

$V_{0.5}$ and slope factor values for $Ca_V1.2$ and mutants in barium and calcium. Data were fit using the equation $I = G_{max} * (V_m - V_{rev})/(1 + \exp(V_{0.5} - V_m)/K_a)$, where I is the measured peak current at each V_m, G_{max} is the maximal conductance, V_m is the test potential, V_{rev} is the reversal potential, $V_{0.5}$ is the midpoint of activation, and K_a is the slope factor (Kanevsky and Dascal, 2006). n-values are identical to the values for equivalent constructs in Table I.

about an approximately sixfold increase in t_{i300} (36.9 ± 4.1% vs. 6.5 ± 1.3%, respectively), a comparable effect relative to that observed in $Ca_V1.2$ GGG. Substitution of six glycines, denoted as $Ca_V2.1$ 6G, gave rise to channels with VDI properties similar to $Ca_V2.1$ GGG, indicating that as in the $Ca_V1.2$ case, an IS6-AID linker triple-glycine substitution is sufficient for uncoupling the VDI modulatory effects of $Ca_V\beta_{2a}$ from the pore-forming subunit. Alanine substitution at the same positions, $Ca_V2.1$ AAA and $Ca_V2.1$ 6A, only had marginal effects on VDI, suggesting that none of the side chains deleted by the multiple glycine substitutions was responsible for the VDI acceleration. Collectively, the data indicate that an intact IS6-AID linker helix is essential for $Ca_V\beta_{2a}$-dependent modulation of Ca_V1 and Ca_V2 VDI.

Glycine Substitutions Disrupt the Ability of the IS6-AID Linker to Form an α-Helix

To determine the structural consequences of our substitutions in the IS6-AID linker, we examined the secondary structure content of peptides corresponding to $Ca_V1.2$ wild-type, AAA, and GGG IS6-AID linkers (Fig. 2 A). Under aqueous conditions, CD experiments indicated that the helical contents of all three versions of the IS6-AID linker are low, <10% (Fig. 2 A). To reveal whether the substitutions affect the ability of the IS6-AID linker to adopt a helical structure as intended, we measured the effects on the peptide CD spectra caused by the addition of TFE, a solvent that induces helical structure in a manner that reflects polypeptide intrinsic helicogenic properties (Shiraki et al., 1995; Buck, 1998). The CD spectra reveal a gradual acquisition of helical content concomitant with an increase in TFE concentration (Fig. 2 A). Under conditions of maximal TFE concentration (50% TFE), both wild-type and AAA peptides displayed the hallmark double minima associated with α-helical structure (Berova et al., 2000) and helical contents of 72 and 64%, respectively (Fig. 2 B). The slightly diminished amount of helical character in AAA IS6-AID peptide relative to wild type may originate in the loss of the potential stabilizing (i, i+4) ionic interaction (Marqusee and Baldwin, 1987) that could form between lysine 416 and aspartate 420. In contrast, GGG IS6-AID peptide has only 28% helical content under conditions in which the other peptides have reached their maximal helix content (Fig. 2, A and B). These data provide strong support for the idea that the GGG substitution is sufficient to break the helical character of the IS6-AID linker, are in agreement with the effects seen in the CD spectra of similar peptides from $Ca_V.2.2$ (Arias et al., 2005), and strongly suggest that the functional uncoupling we observe between $Ca_V\beta_{2a}$ and $Ca_V1.2$ results from disruption of helical structure in the IS6-AID linker.

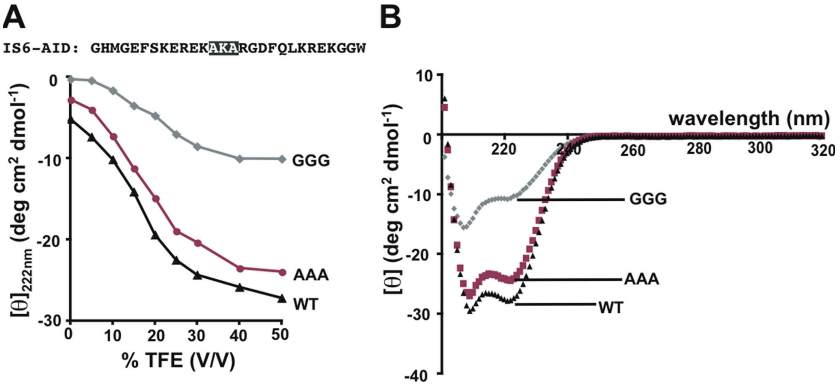

Figure 2. Glycine substitution in IS6-AID linker disrupts helical structure. (A) Mean residue ellipticity at 222 nm for IS6-AID linker peptide, and AAA and GGG mutant peptides as a function of TFE concentration. Peptide sequence is shown. Black highlights the site of the GGG and AAA mutations. (B) IS6-AID linker peptide CD spectra at a peptide concentration of 50 μM in 50% TFE.

Downloaded from http://rupress.org/jgp/article-pdf/133/3/327/1914330/jgp_200810143.pdf by guest on 09 February 2026

Rank Order Effects of $Ca_V\beta$ Isoforms Remain in the Presence of Disrupted IS6-AID Linker

Prior studies of VDI rates imparted to $Ca_V\alpha_1$ subunits by various $Ca_V\beta$ isoforms demonstrated a stereotyped rank order: fastest to slowest, $Ca_V\beta_1 > Ca_V\beta_{2b} > Ca_V\beta_{2a}$ (Olcese et al., 1994; Stea et al., 1994; De Waard and Campbell, 1995; Yasuda et al., 2004). Coexpression of $Ca_V1.2$ with $Ca_V\beta_1$, $Ca_V\beta_{2b}$, or $Ca_V\beta_{2a}$ results in VDI that is 3.2- and 1.3-fold faster for $Ca_V\beta_1$ and $Ca_V\beta_{2b}$ relative to $Ca_V\beta_{2a}$ (Fig. 3 A and Table I). Additionally, the mutant subunit $ssCa_V\beta_{2a}$ (Chien et al., 1996), which lacks the N-terminal palmitoylation that causes $Ca_V\beta_{2a}$ to retard VDI (Chien and Hosey, 1998; Qin et al., 1998; Restituito et al., 2000), displays VDI that is 1.8-fold faster than $Ca_V\beta_{2a}$ and similar to $Ca_V\beta_{2b}$.

Having established that different $Ca_V\beta$ subunits impart stereotyped VDI differences to $Ca_V1.2$, and that GGG causes a clear acceleration of $Ca_V1.2$ VDI in the presence of $Ca_V\beta_{2a}$ (Fig. 1 B), we investigated how the GGG mutation affected the VDI modulation of $Ca_V1.2$ by the different $Ca_V\beta$ isoforms. $Ca_V1.2$ GGG channels coexpressed with $Ca_V\beta_1$, $Ca_V\beta_{2b}$, or $ssCa_V\beta_{2a}$ all have greatly accelerated VDI compared with wild-type $Ca_V1.2$ coexpressed with the same isoforms (VDI τ value increases of 5.6-, 10.7-, and 7.8-fold for $Ca_V\beta_1$, $Ca_V\beta_{2b}$, and $ssCa_V\beta_{2a}$, respectively) (Fig. 3, A and B, and Table I). Interestingly, the rank order VDI effects relative to $Ca_V\beta_{2a}$ are retained (2.4-, 1.8-, and 1.9-fold faster for $Ca_V\beta_1$, $Ca_V\beta_{2b}$, and $ssCa_V\beta_{2a}$ relative to $Ca_V\beta_{2a}$). Similar experiments using wild-type $Ca_V2.1$, $Ca_V2.1$ GGG, $Ca_V\beta_1$, and $Ca_V\beta_{2a}$ show that the GGG substitution causes $Ca_V2.1$ channels to inactivate considerably faster regardless of the $Ca_V\beta$ isoform while also maintaining the isoform-specific rank order (Fig. 3 C). The retention of the relative VDI rank order in the context of disrupted Ca_V1 and Ca_V2 IS6-AID linkers suggests the existence of conserved secondary interaction sites between $Ca_V\beta$ and yet to be defined regions of the pore-forming subunits. The observation that $Ca_V1.2$ GGG and $Ca_V2.1$ GGG channels both inactivate faster than wild type regardless of the $Ca_V\beta$ isoform provides further support for the idea that the IS6-AID linker forms a rigid connection that couples $Ca_V\beta$ to the pore. Thus, the importance of the integrity of the IS6-AID linker for $Ca_V\beta$ modulation of VDI is a common element of high voltage–activated $Ca_V\alpha_1$ architecture.

Disruption of IS6-AID Linker or $Ca_V\beta$ Binding Reduces CDI

Given the clear effects of IS6-AID linker disruption on VDI, we investigated whether disruption of the IS6-AID linker affected the other prominent mode of Ca_V inactivation, CDI. When calcium ions are used as the charge carriers, the time-dependent decay of Ca_V currents arises from two processes: CDI and VDI, which is calcium independent. As long as CDI is much faster than VDI, apparent changes in inactivation of Ca_V calcium currents caused by the presence of different subunits or resulting from mutations should reflect alteration of the actual extent of inactivation driven by calcium-dependent feedback modulation. However, when CDI and VDI occur on similar timescales, the observed inactivation represents contributions from both processes and can confound the analysis. Measurement of the ratio of I_{Ca} and I_{Ba} from the same cell permits one to separate CDI

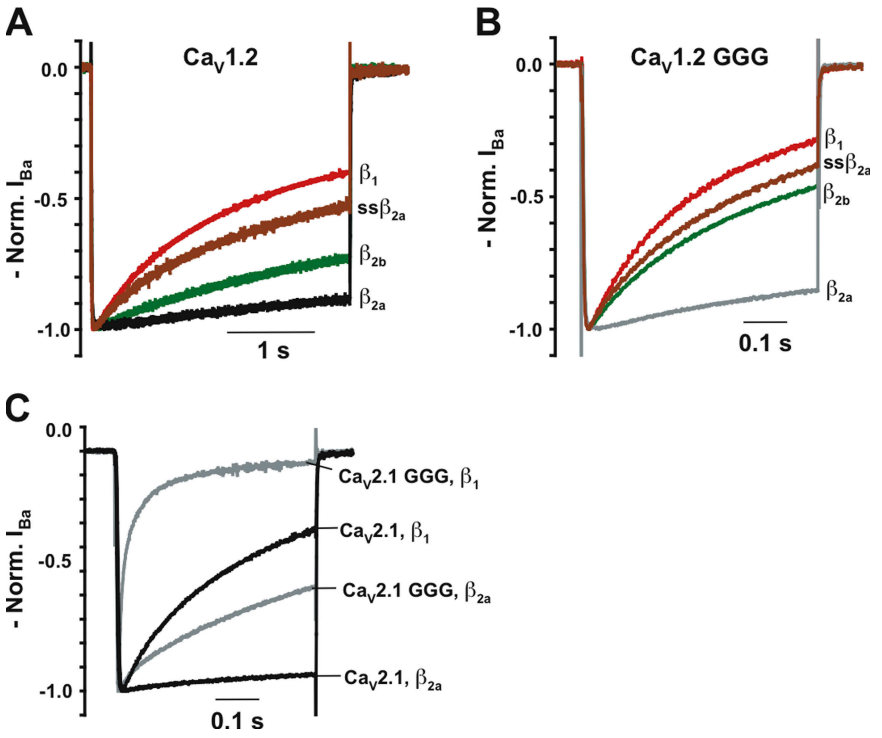

Figure 3. $Ca_V\beta$ isoform rank order VDI effects remain in the presence of disrupted IS6-AID linker. Representative normalized I_{Ba} traces for the indicated $Ca_V\beta$ subunits coexpressed with (A) $Ca_V1.2$ and (B) $Ca_V1.2$ GGG. Note the different timescales. (C) Representative normalized I_{Ba} traces for coexpression of $Ca_V\beta_1$ and $Ca_V\beta_{2a}$ with $Ca_V2.1$ and $Ca_V2.1$ GGG.

Downloaded from http://rupress.org/jgp/article-pdf/133/3/327/1914330/jgp_200810143.pdf by guest on 09 February 2026

and VDI contributions. Division of normalized I_{Ca}, which measures inactivation by CDI and VDI, by normalized I_{Ba}, which reflects the fraction of channels available to undergo inactivation, yields a ratio that isolates the contribution of calcium-dependent processes to the overall observed inactivation (Barrett and Tsien, 2008). The more common practice of taking the simple difference between CDI and VDI can underestimate effects on CDI when VDI is accelerated, a problem that the normalized I_{Ca}/I_{Ba} metric avoids. Because many of our manipulations accelerate VDI, we used the normalized I_{Ca}/I_{Ba} metric, which we denote as netCDI, to analyze the inactivation properties of the mutant channels.

A previous study of wild-type $Ca_V1.2$ channels expressed in a mammalian cell line suggested that in some cases, I_{Ba} may also undergo current-dependent inactivation (Ferreira et al., 1997), a condition that if present to a substantial degree would complicate the netCDI analysis. To test whether such a phenomenon occurred in our *Xenopus* oocyte experimental setup, we examined the inactivation properties of I_{Ba} using a double-pulse protocol (Fig. 4 C). Comparison of the I_{Ba} prepulse and test pulse amplitudes does not reveal a U-shaped dependence that would be a signature of VDI current-dependent inactivation (Fig. 4 C) and supports the use of netCDI as a means for parsing inactivation into effects from CDI and VDI.

In striking contrast to the VDI acceleration caused by the IS6-AID linker GGG mutation, two-electrode voltage clamp experiments in *Xenopus* oocytes in which calcium ions were used as the charge carrier showed that the GGG mutation unexpectedly decreased netCDI (Fig. 4 A and Table I). The triple-glycine mutation caused drastic reductions relative to wild type in both the main inactivating component (τ_1 = 217 ± 16 ms vs. 20.3 ± 4.2 ms, respectively) and extent of inactivation, t_{i300} (43.7 ± 3.6% vs. 69.5 ± 2.6%) (Fig. 4, A and B, and Table I). Unlike the VDI case in which GGG and 6G substitutions had equivalent effects on inactivation, $Ca_V1.2$ 6G showed a further reduction in netCDI extent (t_{i300} =19.8 ± 5.4%), although the time constant of the main inactivating component was not changed. A similarly strong reduction of netCDI

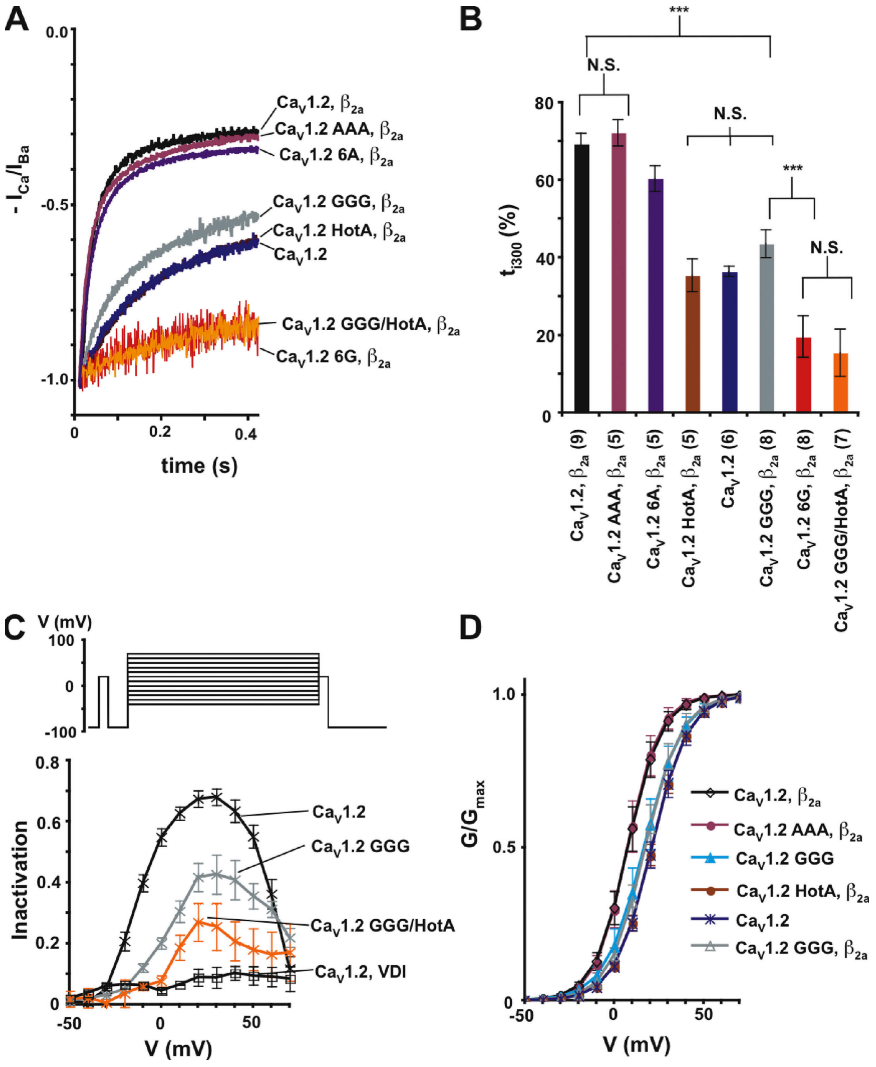

Figure 4. IS6-AID linker disruption reduces CDI. (A) Representative netCDI (I_{Ca}/I_{Ba}) at a test potential of +20 mV for the combinations of the indicated $Ca_V1.2$ subunits and $Ca_V\beta_{2a}$. (B) t_{i300} values from A. Results of unpaired *t* tests are indicated as follows: N.S., $P > 0.05$, not significant; ***, $P < 0.001$. (C) Isochronal inactivation of $Ca_V1.2$ ($n = 4$, black X's, netCDI; $n = 4$, black open squares, VDI), $Ca_V1.2$ GGG netCDI ($n = 4$, gray), and $Ca_V1.2$ GGG/HotA netCDI ($n = 5$, orange). Inactivation extent comparing the ratio of prepulse and test pulse current amplitudes plotted as a function of the test voltage. The pulse protocol is shown at the top. (D) G-V relationships in calcium for the indicated combinations of $Ca_V1.2$ subunits and $Ca_V\beta_{2a}$.

Downloaded from http://rupress.org/jgp/article-pdf/133/3/327/1914330/jgp_200810143.pdf by guest on 09 February 2026

extent was seen in the GGG/HotA mutant (Fig. 4 A). In contrast to the potent changes elicited by the glycine substitutions, $Ca_V1.2$ AAA and $Ca_V1.2$ 6A netCDI were very similar to wild type (Fig. 4 A and Table I). The $Ca_V1.2$ 6G and $Ca_V1.2$ GGG/HotA mutants expressed at lower levels than most other mutant channels (Table S2). To test the possibility that the additional reduction in netCDI observed in these cases was due to an indirect effect caused by the low current amplitudes, we recorded wild-type $Ca_V1.2$ currents at comparable expression levels (Fig. S5). Comparison of these currents showed no change in netCDI. Thus, the changes in netCDI can be confidently attributed to direct effects on the channel that arise from the mutations and not from differences in current amplitudes.

To examine the changes to netCDI over a broad voltage range, we measured netCDI using a multi-pulse protocol in which the extent of inactivation was measured following a variable voltage pulse and compared with a control prepulse (Fig. 4 C). Under this protocol, wild-type $Ca_V1.2$ netCDI displays the typical inverted U-shape dependence expected of a calcium-dependent modulatory process. This dependence is markedly reduced for both $Ca_V1.2$ GGG and $Ca_V1.2$ GGG/HotA (Fig. 4 C). The drastic reduction in the U-shape dependence of inactivation in the mutant channels adds further support for the idea that the IS6-AID linker and $Ca_V\beta$ have a role in CDI.

Comparison of netCDI measured from $Ca_V1.2$ coexpressed with $Ca_V\beta_{2a}$, $Ca_V1.2$ expressed without $Ca_V\beta$, and $Ca_V1.2$ HotA, which cannot bind $Ca_V\beta$, revealed an unexpected effect of $Ca_V\beta_{2a}$. $Ca_V\beta_{2a}$ causes a dramatic, ~10-fold increase in netCDI (τ_1 = 20.3 ± 4.2 ms, 216 ± 55 ms, and 239 ± 42 ms, respectively) (Fig. 4 A and Table I). This netCDI acceleration stands in stark disparity to the approximately eightfold retardation $Ca_V\beta_{2a}$ imparts to VDI relative to channels lacking $Ca_V\beta$. Hence, $Ca_V\beta_{2a}$ has the opposite functional effects on CDI and VDI. This paradoxical effect has not been noted previously. netCDI for $Ca_V1.2$ GGG channels coexpressed with $Ca_V\beta_{2a}$ is indistinguishable from $Ca_V1.2$ channels expressed in the absence of a $Ca_V\beta$ subunit and HotA channels that cannot bind $Ca_V\beta$ (τ_1 = 217 ± 16 ms, 216 ± 55 ms, and, 239 ± 42 ms, respectively). Thus, even though the GGG mutation has opposite effects on $Ca_V\beta_{2a}$-mediated VDI and CDI, accelerating the former while decelerating the latter, the net effect is the same. The $Ca_V1.2$ GGG channels inactivate with τ values equivalent to channels lacking $Ca_V\beta_{2a}$ modulation.

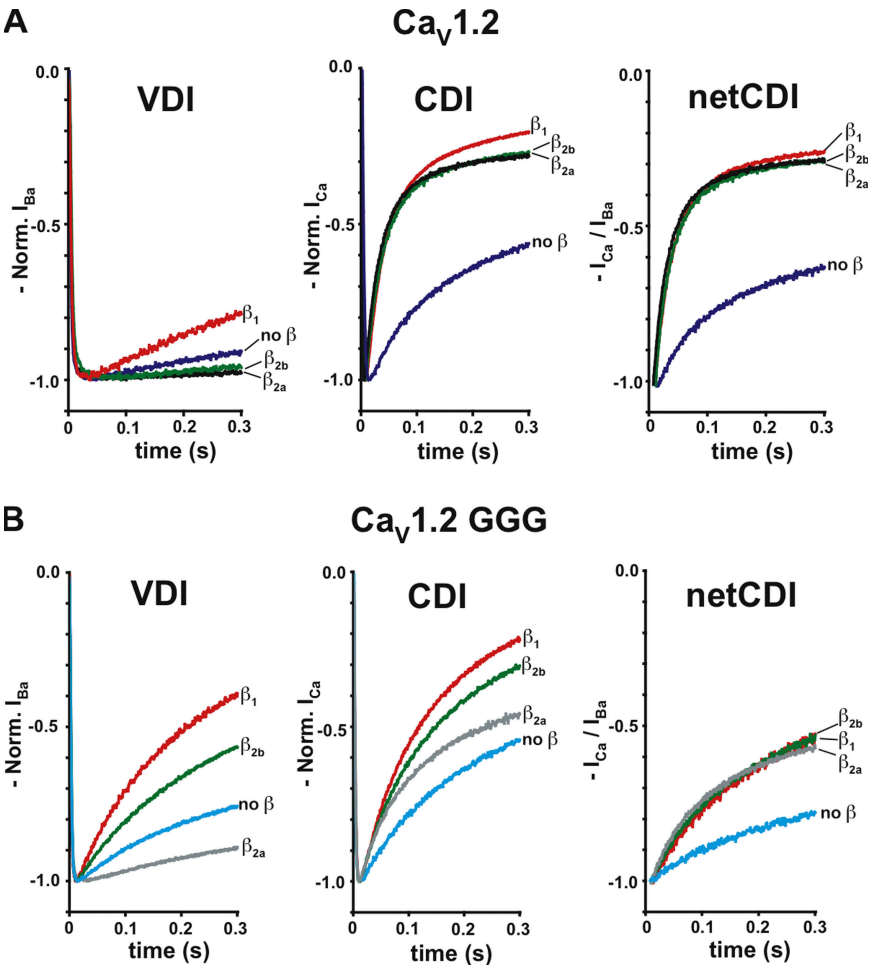

Figure 5. Effects of $Ca_V\beta$ isoforms on calcium inactivation stem from underlying effects on VDI. Normalized inactivation curves measured at +20 mV for (A) $Ca_V1.2$ and (B) $Ca_V1.2$ GGG subunits coexpressed with $Ca_V\beta_1$, $Ca_V\beta_{2a}$, $Ca_V\beta_{2b}$, or in the absence of $Ca_V\beta$. (Left) VDI is shown and is reproduced for comparison from the first 300 ms of Fig. 3 (A and B). (Middle) Inactivation in calcium. (Right) netCDI.

Downloaded from http://rupress.org/jgp/article-pdf/133/3/327/1914330/jgp_200810143.pdf by guest on 09 February 2026

Similar to the effect seen using barium as a charge carrier, the use of calcium as the charge carrier reveals that $Ca_V1.2$ GGG lacks the hyperpolarizing shift in the G-V relationship caused by $Ca_V\beta_{2a}$ (Fig. 4 D, Fig. S3 B, and Table II). Further, the $Ca_V1.2$ GGG/$Ca_V\beta_{2a}$ channels show similar G-V relationships to wild-type $Ca_V1.2$ expressed in the absence of $Ca_V\beta$ and to $Ca_V1.2$ HotA. In contrast, $Ca_V1.2$ AAA coexpressed with $Ca_V\beta_{2a}$ behaves like wild-type $Ca_V1.2$ (Fig. 4 D). Therefore, disruption of the IS6-AID linker shows similar abrogation of effects on voltage activation caused by $Ca_V\beta_{2a}$, regardless of the divalent charge carrier.

Together with the data from the studies of IS6-AID linker peptides, the results strongly suggest that the observed reduction in netCDI for $Ca_V1.2$ GGG and $Ca_V1.2$ 6G is the consequence of the disruption of the IS6-AID linker. These data provide compelling evidence that both $Ca_V\beta$ and an intact IS6-AID linker are required for netCDI and suggest that there is an intimate dependence between elements that drive CDI, namely the Ca^{2+}–CaM-IQ domain complex (Halling et al., 2006), and components that control VDI.

$Ca_V\beta$ Isoform Identity Has Little Influence on $Ca_V1.2$ netCDI

In light of the clear rank order effects that different $Ca_V\beta$ isoforms have on VDI, we asked whether there were similar differences in netCDI when different $Ca_V\beta$s were present. Wild-type $Ca_V1.2$ channels coexpressed with $Ca_V\beta_1$, $Ca_V\beta_{2a}$, or $Ca_V\beta_{2b}$ show small differences in CDI but no real difference when netCDI is considered (τ values of 20–30 ms) (Fig. 5 A and Table I). Incorporation of the triple-glycine mutant in the $Ca_V1.2$ IS6-AID linker causes a reduction in CDI in the presence of $Ca_V\beta_1$, $Ca_V\beta_{2b}$, and $Ca_V\beta_{2a}$ (τ_1 = 200–350 ms; Table I). Even though there appear to be differences between the $Ca_V\beta$ isoforms with respect to inactivation in calcium (Fig. 5 B, middle, and Table S1), these distinctions are due almost exclusively to the underlying VDI differences (Fig. 5 B, left) and vanish when one considers netCDI (Fig. 5 B, right, and Table I). Together with the HotA CDI results, these data suggest that although a $Ca_V\beta$ subunit is required for CDI, all $Ca_V\beta$ isoforms support netCDI equally. Thus, the primary route for coupling CDI components to the pore would appear to be through the IS6-AID linker and not through secondary interactions sites that contribute to isoform-specific VDI modulation differences.

CDF Is Reduced by Disruption of Either IS6-AID Linker or $Ca_V\beta$ Association

$Ca_V1.2$ channels display a phenomenon known as CDF, which is unmasked in the context of a point mutation, I1624A, in the C-terminal tail IQ domain that comprises the primary Ca^{2+}/CaM binding site (Zühlke et al., 1999, 2000; Hudmon et al., 2005; Van Petegem et al., 2005). Given the pronounced effects of the IS6-AID linker GGG mutation and the importance of $Ca_V\beta$ for both VDI and CDI, we tested whether CDF might also rely upon an intact IS6-AID linker or the $Ca_V\beta$ subunit. Under conditions of similar current amplitude, the GGG mutation causes a reduction in $Ca_V1.2$ I1624A CDF of almost two thirds (13.8 ± 8.2% GGG/I1624A vs. 38.9 ± 12.3% I1624A, respectively). In contrast, the corresponding AAA mutant

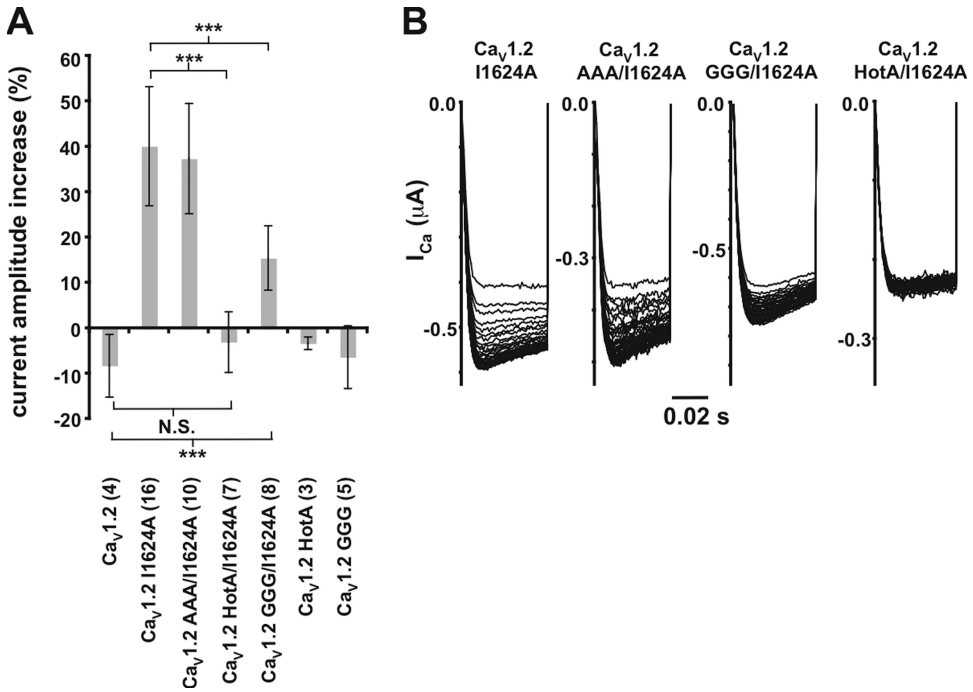

Figure 6. CDF is reduced by disruption of the IS6-AID linker and loss of $Ca_V\beta$ binding. (A) Relative current increase between the last (40th) and first +20-mV pulses at 3 Hz for $Ca_V1.2$ and the indicated mutants. Parentheses indicate the number of oocytes tested. Results of unpaired *t* tests are indicated as follows: N.S., $P > 0.05$, not significant; ***, $P < 0.001$. (B) Exemplar current traces for $Ca_V1.2$ I1624A, $Ca_V1.2$ GGG/I1624A, and $Ca_V1.2$ HotA/I1624A in a 3-Hz 40-pulse train normalized to the peak of the first pulse.

Downloaded from http://rupress.org/jgp/article-pdf/133/3/327/1914330/jgp_200810143.pdf by guest on 09 February 2026

did not alter CDF significantly (37.5 ± 12.1%). $Ca_V1.2$ I1624A channels incapable of binding $Ca_V\beta$ through the incorporation of the HotA mutations show a complete absence of CDF (Fig. 6). This result agrees with the observation that $Ca_V\beta$ is central to the CDF mechanism (Grueter et al., 2006). Collectively, these data suggest that CDF requires both an intact IS6-AID linker and a $Ca_V\beta$ subunit, and that both $Ca_V1.2$ netCDI and CDF use the same components, including the IS6-AID linker and $Ca_V\beta$ for communicating with the transmembrane pore.

DISCUSSION

The process of inactivation is critical for Ca_V function and forges important connections between electrical signaling, activity-dependent feedback modulation of the channel, and activation of other calcium-dependent signaling cascades. Although a definitive molecular mechanism has yet to emerge, several models have been forwarded for how the components that govern the two principal inactivation processes, VDI and CDI, communicate with the transmembrane pore to regulate inactivation. The models fall into two distinct classes: those that assert that VDI and CDI use the same physical components to regulate the open state of the transmembrane pore (Cens et al., 1999; Stotz and Zamponi, 2001; Soldatov, 2003; Findlay, 2004; Kim et al., 2004), and those that maintain VDI and CDI use distinct physical components (Lee et al., 1985; Hadley and Lederer, 1991; Barrett and Tsien, 2008).

Identification of elements that affect VDI is relatively straightforward. Examination of the consequences of mutational manipulations or changes in subunit composition for inactivation when barium is the permeant ion provides an unambiguous VDI metric. Consequently, characterization of mutations in various elements of the $Ca_V1.2$ C terminus including the IQ domain, which has a prominent role in CDI (Zühlke et al., 1999; Barrett and Tsien, 2008), putative EF-hand, and sequences between IQ domain and EF-hand (Zühlke and Reuter, 1998; Kim et al., 2004), have indicated that many components that are thought to be important for CDI also affect VDI.

On the contrary, delineation of the extent to which components that are thought to dominate VDI, such as the $Ca_V\beta$/I-II loop complex (Olcese et al., 1994; Stea et al., 1994; De Waard and Campbell, 1995), contribute to inactivation under conditions when calcium is the permeant ion can be problematic. In the regime where VDI and CDI occur on the same timescale, perturbation to elements that contribute to VDI may also alter apparent CDI rates. Such changes might lead one to mistakenly conclude that VDI components have a role in CDI and that perhaps both inactivation processes use common elements. This point has been clearly articulated recently by Barrett and Tsien (2008), who present a new and important means of analyzing Ca_V inactivation that allows for a dissection of the relative contributions of VDI and CDI to the overall inactivation process. The calculation of the normalized I_{Ca}/normalized I_{Ba} ratio (Barrett and Tsien, 2008), a parameter we call netCDI, allows the isolation of the inactivation component that is specifically conferred by calcium and avoids complications that could be caused by acceleration of VDI. This type of analysis indicates that prior evidence used to support the idea of a shared role for $Ca_V\beta$ action in VDI and CDI (Cens et al., 1999) can be explained entirely by differences in how the different $Ca_V\beta$s act on VDI (Barrett and Tsien, 2008) (compare Fig. 5 A). Thus, whether CDI requires the VDI components or proceeds via an independent mechanism has remained an open question.

Structural Integrity of the IS6-AID Linker Is Essential for VDI and CDI

Our experiments testing the importance of the structural integrity of the IS6-AID linker support the idea that in Ca_V1 and Ca_V2 channels, the IS6-AID linker is a helix that functions as a rigid rod connecting $Ca_V\beta$ to the pore domain (Opatowsky et al., 2004; Van Petegem et al., 2004; Arias et al., 2005) (Fig. 7 A). This structural connection appears to be responsible for a large fraction of the VDI modulation that any $Ca_V\beta$ isoform imparts on $Ca_V\alpha_1$ subunits and for the effects $Ca_V\beta$ has on channel activation (compare Figs. 1 and 4).

X-ray crystallographic (Chen et al., 2004; Opatowsky et al., 2004; Van Petegem et al., 2004) and CD studies (Opatowsky et al., 2004; Van Petegem et al., 2008) indicate that the helical structure of the AID, which is integral to the $Ca_V\alpha_1$–$Ca_V\beta$ interaction, is induced by formation of the AID–$Ca_V\beta$ complex. The presence of such a well-supported helix and consideration of the established importance of such a template for nucleating helix formation (Zimm and Bragg, 1959; Lifson and Roig, 1961; Wang et al., 2006; Patgiri et al., 2008) suggest that the AID helix can promote the propagation of α-helical structure in the IS6-AID linker (Opatowsky et al., 2004; Van Petegem et al., 2004). In agreement with this hypothesis, we find that mutations that reduce the helical propensity of the IS6-AID linker and mutations that eliminate $Ca_V\beta$ binding to the AID have similar functional effects.

Remarkably, we find that disruption of the IS6-AID linker by the GGG mutation or the loss of $Ca_V\beta$ binding caused by the disruption of the AID-binding hotspot by the HotA mutations (Van Petegem et al., 2008) also causes large reductions (>10-fold) in the main inactivation component of netCDI. The remaining netCDI can be essentially eliminated by the introduction of additional flexibility into the IS6-AID linker ($Ca_V1.2$ 6G) or by the GGG/HotA combination (Fig. 4). These data constitute strong evidence that CDI relies on $Ca_V\beta$ and portions of the I-II loop, physical components that have been traditionally associated with VDI.

Interestingly, the disruption of the IS6-AID linker structural integrity affects VDI and CDI in opposite directions;

Downloaded from http://rupress.org/jgp/article-pdf/133/3/327/1914330/jgp_200810143.pdf by guest on 09 February 2026

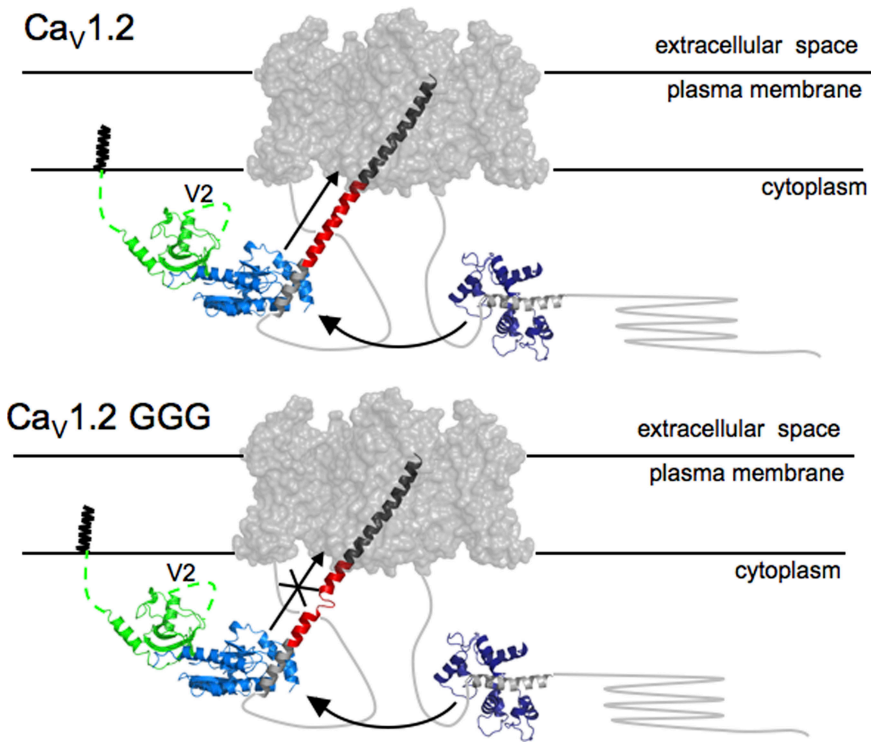

Figure 7. Cartoon model of a Ca_V channel. Based on the likely gross similarly between Ca_V and Kv transmembrane portions, the Kv1.2 transmembrane domains (gray surface; PDB accession no. 2A79) are used to represent the Ca_V transmembrane domains. The IS6-AID linker (red) was modeled manually by building a helix of corresponding length between the Kv1.2 S6 helix C terminus (dark gray) and AID helix (light gray) from the $Ca_V\beta_{2a}$–AID complex (PDB accession no. 1T0J). The $Ca_V\beta_{2a}$–AID complex is shown as follows: green, SH3 domain; light blue, NK domain; light gray, AID. N-terminal $Ca_V\beta_{2a}$ variable segment, V1, of unknown structure, is shown anchored to the membrane via N-terminal palmitoylation, and the V2 loop is indicated. Arrow along the IS6-AID linker indicates communication between $Ca_V\beta$ and the pore domain. This is lost in the multiple glycine mutants (bottom) and affects VDI, CDI, and CDF. Curved arrow between the Ca^{2+}/CaM-IQ domain complex (PDB accession no. 2BE6), Ca^{2+}/CaM (dark blue), and IQ helix (gray) represents the functional interaction between the C-terminal tail complex and the $Ca_V\beta_{2a}$–AID complex required for CDI and CDF. In $Ca_V1.2$ GGG (bottom), IS6-AID helix disruption blunts the influence of the Ca^{2+}/CaM-IQ domain on the transmembrane pore.

VDI is accelerated, while CDI is slowed down. By use of the netCDI analysis, we uncovered a previously unrecognized difference between how $Ca_V\beta_{2a}$ affects VDI and CDI. $Ca_V\beta_{2a}$, which slows VDI relative to channels lacking a $Ca_V\beta$ subunit (Olcese et al., 1994; Stea et al., 1994) (Fig. 1 B), accelerates netCDI (Fig. 4 A). These changes mirror the seemingly opposite effects of the GGG mutation on VDI and CDI in the presence of $Ca_V\beta_{2a}$. Thus, the VDI and CDI results are both consistent with the same interpretation; a rigid IS6-AID linker is absolutely required to couple $Ca_V\beta$ with the pore and indicate that $Ca_V\beta$ has a centrally important role in CDI.

Our data support the hypothesis that VDI and CDI act through shared components (Cens et al., 1999; Stotz and Zamponi, 2001; Soldatov, 2003; Findlay, 2004; Kim et al., 2004) rather than through independent elements (Lee et al., 1985; Hadley and Lederer, 1991; Barrett and Tsien, 2008). The observation that VDI proceeds through a process that includes gating charge immobilization whereas CDI does not has given support to the idea that VDI and CDI are mediated by distinct effector mechanisms (Barrett and Tsien, 2008) and would seem at odds with the interpretation that both VDI and CDI act through a common element, namely $Ca_V\beta$ and the IS6-AID linker. However, our discovery that $Ca_V\beta_{2a}$ has opposite effects on VDI and CDI may provide a way to reconcile this observation. It suggests that the underlying structural rearrangements that cause VDI and CDI are not equivalent, even though both rely upon the coupling of $Ca_V\beta$ to the pore via a rigid IS6-AID linker. Further support for this idea comes from the observations that the different $Ca_V\beta$ isoforms have dissimilar effects on VDI but not netCDI (Fig. 5), and that relative to the GGG mutation, GGG/HotA affects netCDI but not VDI (Fig. 4 and Table I).

How Do VDI and CDI Elements Communicate?

The functional evidence that the main VDI and CDI elements operate in an interdependent manner raises the question about the exact underlying molecular interactions that drive VDI and CDI. The simplest hypothesis is that, at least in one functional state, there is a direct physical interaction between the two major components of VDI and CDI, the $Ca_V\beta/Ca_V\alpha_1$-I-II loop and Ca^{2+}/CaM/$Ca_V\alpha_1$–C-terminal tail complexes. Unfortunately, robust evidence for such a direct physical interaction remains elusive. Pulldown experiments by Kim et al. (2004) have suggested that there could be an interaction between the isolated I-II loop and the $Ca_V1.2$ C terminus; however, those experiments were done in the absence of $Ca_V\beta$, conditions under which the AID portion of the I-II loop is not folded (Opatowsky et al., 2004; Van Petegem et al., 2008). Therefore, whether the observed interaction reflects authentic binding between

Downloaded from http://rupress.org/jgp/article-pdf/133/3/327/1914330/jgp_200810143.pdf by guest on 09 February 2026

two natively folded components remains an open question. Using a similar assay, Zhang et al. (2005) reported the binding of $Ca_V\beta$ to the $Ca_V1.2$ C terminus; however, this interaction was preserved even when a mutant construct that destroys $Ca_V\beta$ structural integrity, the ΔBID mutant, was used. Thus, the observed $Ca_V\beta$–$Ca_V1.2$ C terminus interaction cannot reflect a functionally relevant interaction. Our attempts to establish robust complexes between biochemically well-behaved constructs that include $Ca_V\beta$, the I-II loop, and the C-terminal complex having defined stoichiometries have thus far been unsuccessful.

Even though the functional data indicate a codependency between the $Ca_V\beta$/I-II loop and the calcium-sensing elements of the channel, such a functional link does not demand a direct physical association of these components. Given the substantial amount of Ca_V mass in the cytoplasm, ∼150 kD (Van Petegem and Minor, 2006), and that the $Ca_V\beta/Ca_V\alpha_1$-I-II loop and $Ca^{2+}/CaM/Ca_V\alpha_1$–C-terminal tail complexes comprise only a portion of this mass, it seems likely that interactions between the $Ca_V\beta/Ca_V\alpha_1$-I-II loop and $Ca^{2+}/CaM/Ca_V\alpha_1$–C-terminal tail complexes involve other yet to be determined elements from the pore-forming subunit intracellular portions. One candidate is the N-terminal cytoplasmic domain (Ivanina et al., 2000; Dick et al., 2008; Tadross et al., 2008). Defining the exact arrangement of the channel intracellular components and the state dependence of interactions between the $Ca_V\beta$/I-II loop and CaM/C-terminal complexes remains an important goal. Further, it will be essential to determine how rearrangements within the channel cytoplasmic domains affect changes in the pore that may also participate in channel inactivation (Babich et al., 2007).

Effects of IS6-AID Linker Disruption on VDI and CDI Are Incompatible with a Hinged Lid Model

The details of the macromolecular conformational changes that cause Ca_V inactivation remain unknown. To account for the importance of the I-II linker in determining inactivation rates of Ca_V channels and chimaeras (Cens et al., 1999; Stotz et al., 2000), Ca_V inactivation has been suggested to occur via an inactivation particle or hinged lid analogous to voltage-gated sodium channels (Goldin, 2003; Ulbricht, 2005). The N-terminal portion of the AID helix has been suggested as a candidate for a Ca_V inactivation particle (Dafi et al., 2004) based on the influence that charged residues on the AID external face in the $Ca_V\beta$–AID complex have on VDI kinetics (Herlitze et al., 1997; Berrou et al., 2001; Dafi et al., 2004).

From the homology and deep evolutionary relationship between Ca_Vs and voltage-gated potassium channels (Hille, 2001), it is very likely that Ca_V IS6 is a helical pore-lining segment similar to the homologous region of voltage-gated potassium channels (Long et al., 2005). Our data indicate that the IS6-AID linker forms a continuous helix that bridges the AID helix and IS6. To assess the impact of such a structural element on the probable location of the $Ca_V\beta$–AID complex relative to the pore, we modeled a helical IS6-AID linker onto the structure of the Kv1.2 transmembrane domains (Long et al., 2005). The resulting continuous helix places the $Ca_V\beta$–AID complex ∼40 Å distant from the pore (Fig. 7). This structural arrangement is incompatible with a mechanism in which the $Ca_V\beta$–AID acts as an inactivation particle that approaches the pore. The glycine substitutions that we tested are situated midway between the pore and $Ca_V\beta$–AID complex and should impart increased flexibility to the IS6-AID linker. If the $Ca_V\beta$–AID complex acted like an inactivation particle that needed to approach the pore, these substitutions would be expected to show a minimal effect. In contrast, we see greatly increased inactivation τ values (Figs. 1 and 3). Further, the absence of effects on inactivation in the case where no $Ca_V\beta$ is bound (e.g., $Ca_V1.2$ GGG-$Ca_V\beta_{2a}$ vs. $Ca_V1.2$ GGG/HotA-$Ca_V\beta_{2a}$), and where the helix propensity of the IS6-AID linker is increased by multiple alanine substitutions, also conflicts with the idea that there is some sort of inactivation particle formed by the $Ca_V\beta$–AID complex. Thus, it seems difficult to reconcile the functional effects of the IS6-AID linker mutations with the I-II linker acting as a hinged lid or inactivation particle. Rather, our results support the idea that inactivation involves some type of constriction of the pore involving the S6 segments from each domain (Zhang et al., 1994; Stotz et al., 2000; Cens et al., 2006).

A Second Interaction Site between $Ca_V\beta$ and $Ca_V\alpha_1$ Is Important for VDI

The functional consequences of disrupting the helicity of the IS6-AID linker suggest that $Ca_V\beta$s modulate VDI through two different routes. The principal mechanism appears to be through the IS6-AID linker as the changes in τ values caused by the GGG substitution are of the same magnitude as that caused by the absence of a $Ca_V\beta$ subunit (Table I). The fact that the rank order VDI effects of different $Ca_V\beta$ isoforms persists in the context of a disabled IS6-AID linker (Fig. 3) indicates that the IS6-AID linker is not the sole element involved. The palmitoylation of the N-terminal variable domain of $Ca_V\beta_{2a}$ remains an important factor that sets $Ca_V\beta_{2a}$ apart from the other $Ca_V\beta$s. Additionally, there must be other functionally important sites of interaction between $Ca_V\beta$ and other portions of the pore-forming subunit that account for the remnant differences observed among the $Ca_V\beta$s. One candidate for such interactions is the $Ca_V\beta$ V2 (or HOOK) domain, which connects the highly conserved SH3 and NK domains (Hanlon et al., 1999; Chen et al., 2004; Opatowsky et al., 2004; Van Petegem et al., 2004). Indeed, functional experiments support an important role for the V2 region in VDI. Chimeras that swap the V2 region between the core domains of $Ca_V\beta_1$ and $Ca_V\beta_{2a}$ result in an exchange of VDI

Downloaded from http://rupress.org/jgp/article-pdf/133/3/327/1914330/jgp_200810143.pdf by guest on 09 February 2026

properties (He et al., 2007), and deletion of the $Ca_V\beta_{2a}$ V2 domain causes acceleration of VDI (Richards et al., 2007). Our experiments show that $ssCa_V\beta_{2a}$ and $Ca_V\beta_{2b}$ do not have identical effects on VDI (e.g., 1.4-fold difference in τ; Table I), even though both share identical V2 domains. Thus, other $Ca_V\beta$ variable regions must also play a role in VDI. These two isoforms have multiple differences in the V1 and V3 that must bear the elements that contribute to the differing effects on VDI. In contrast, $Ca_V\beta$ subunit isoform identity has little effect on CDI (Fig. 5), suggesting that interactions between the $Ca_V\beta$-variable regions and pore-forming subunit are not critical for CDI. Although the importance of the variable regions with respect to isoform-specific modulation of VDI seems clear from the perspective of the $Ca_V\beta$ subunit, the target sites on the pore-forming subunit remain unknown. Definition of the functionally relevant $Ca_V\beta$ subunit points of contact on the pore-forming subunit remains an important unresolved issue.

CDF and CDI Share Requirement for $Ca_V\beta$ and Intact IS6-AID Linker

Although the detailed mechanism for $Ca_V1.2$ CDF remains unresolved (Richard et al., 2006), three different macromolecular components appear to contribute: the complex of Ca^{2+}/CaM and the $Ca_V\alpha_1$ C-terminal tail IQ domain (Zühlke et al., 1999; Van Petegem et al., 2005), Ca^{2+}/CaM-dependent kinase II (Anderson et al., 1994; Yuan and Bers, 1994; Hudmon et al., 2005; Grueter et al., 2006; Lee et al., 2006), and $Ca_V\beta$ (Grueter et al., 2006). Our data support the critical role of $Ca_V\beta$ in CDF. Incorporation of the HotA mutations that prevent $Ca_V\beta$ binding (Van Petegem et al., 2008) eliminates the CDF that is unmasked by the I1624A IQ domain mutation (Fig. 6). Furthermore, we uncover a requirement for the IS6-AID linker. Disruption of the IS6-AID linker structure blunts CDF and provides new evidence that an intact rigid connection between the channel pore and $Ca_V\beta$ is also essential for CDF (Fig. 6). Collectively, our data show clearly that CDF and CDI share the same requirements, the presence of a $Ca_V\beta$ subunit and an intact IS6-AID linker, suggesting that these two processes use the same determinants to communicate with the pore.

Calcium influx into excitable cells is tightly regulated by a plethora of different processes. Our data strongly suggest that rearrangements of the intracellular Ca_V domains have effects on inactivation that are mediated by $Ca_V\beta$ through a rigid connection to the IS6 pore helix. Presently, very little is known about how Ca_V intracellular domains interact with each other in open-, closed-, or inactivated-channel states. Development of a true molecular description of Ca_V inactivation will require the definition of the physical intermolecular interactions present in each stage of the channel and how they rearrange. The definition of the central role of the $Ca_V\beta$ subunit for VDI, CDI, and CDF should focus attention on defining how this centrally important channel element interacts with other intracellular domains to modulate activity-dependent feedback modulation of the channel.

We thank Y. Fujiwara, A. Tolia, F. Tombola, and F. Van Petegem for comments on the manuscript; F. Van Petegem for the HotA mutant; G. Pitt (Duke University School of Medicine) for the $Ca_V2.1$ clone; R.W. Tsien (Stanford University School of Medicine) for the $Ca_V\beta_1$ and $Ca_V\beta_{2b}$ clones and for critical advice on the work; and K. Clark for technical assistance.

This work was supported by grants to D.L. Minor from National Institutes of Health-National Heart, Lung and Blood Institute, and American Heart Association, and to F. Findeisen from the American Heart Association. D.L. Minor is an AHA Established Investigator.

Edward N. Pugh Jr. served as editor.

Submitted: 16 October 2008
Accepted: 28 January 2009

REFERENCES

Anderson, M.E., A.P. Braun, H. Schulman, and B.A. Premack. 1994. Multifunctional Ca2+/calmodulin-dependent protein kinase mediates Ca(2+)-induced enhancement of the L-type Ca2+ current in rabbit ventricular myocytes. *Circ. Res.* 75:854–861.

Arias, J.M., J. Murbartian, I. Vitko, J.H. Lee, and E. Perez-Reyes. 2005. Transfer of beta subunit regulation from high to low voltage-gated Ca2+ channels. *FEBS Lett.* 579:3907–3912.

Babich, O., V. Matveev, A.L. Harris, and R. Shirokov. 2007. Ca^{2+}-dependent inactivation of $Ca_V1.2$ channels prevents Gd^{3+} block: does Ca^{2+} block the pore of inactivated channels? *J. Gen. Physiol.* 129:477–483.

Barrett, C.F., and R.W. Tsien. 2008. The Timothy syndrome mutation differentially affects voltage- and calcium-dependent inactivation of CaV1.2 L-type calcium channels. *Proc. Natl. Acad. Sci. USA.* 105:2157–2162.

Berjukow, S., R. Marksteiner, S. Sokolov, R.G. Weiss, E. Margreiter, and S. Hering. 2001. Amino acids in segment IVS6 and beta-subunit interaction support distinct conformational changes during Ca(v)2.1 inactivation. *J. Biol. Chem.* 276:17076–17082.

Bernatchez, G., D. Talwar, and L. Parent. 1998. Mutations in the EF-hand motif impair the inactivation of barium currents of the cardiac alpha1C channel. *Biophys. J.* 75:1727–1739.

Berova, N., K. Nakanishi, and R.W. Woody. 2000. Circular Dichroism: Principles and Applications. 2nd edition. Wiley-VCH, New York. 912 pp.

Berrou, L., G. Bernatchez, and L. Parent. 2001. Molecular determinants of inactivation within the I-II linker of alpha1E (CaV2.3) calcium channels. *Biophys. J.* 80:215–228.

Blaber, M., X.J. Zhang, and B.W. Matthews. 1993. Structural basis of amino acid alpha helix propensity. *Science.* 260:1637–1640.

Buck, M. 1998. Trifluoroethanol and colleagues: cosolvents come of age. Recent studies with peptides and proteins. *Q. Rev. Biophys.* 31:297–355.

Catterall, W.A. 2000. Structure and regulation of voltage-gated Ca2+ channels. *Annu. Rev. Cell Dev. Biol.* 16:521–555.

Cens, T., S. Restituito, S. Galas, and P. Charnet. 1999. Voltage and calcium use the same molecular determinants to inactivate calcium channels. *J. Biol. Chem.* 274:5483–5490.

Cens, T., M. Rousset, J.P. Leyris, P. Fesquet, and P. Charnet. 2006. Voltage- and calcium-dependent inactivation in high voltage-gated Ca(2+) channels. *Prog. Biophys. Mol. Biol.* 90:104–117.

Chen, Y.H., M.H. Li, Y. Zhang, L.L. He, Y. Yamada, A. Fitzmaurice, Y. Shen, H. Zhang, L. Tong, and J. Yang. 2004. Structural basis of

Downloaded from http://rupress.org/jgp/article-pdf/133/3/327/1914330/jgp_200810143.pdf by guest on 09 February 2026

the alpha1-beta subunit interaction of voltage-gated Ca2+ channels. *Nature.* 429:675–680.

Chien, A.J., and M.M. Hosey. 1998. Post-translational modifications of beta subunits of voltage-dependent calcium channels. *J. Bioenerg. Biomembr.* 30:377–386.

Chien, A.J., K.M. Carr, R.E. Shirokov, E. Rios, and M.M. Hosey. 1996. Identification of palmitoylation sites within the L-type calcium channel beta2a subunit and effects on channel function. *J. Biol. Chem.* 271:26465–26468.

Clapham, D.E. 2007. Calcium signaling. *Cell.* 131:1047–1058.

Dafi, O., L. Berrou, Y. Dodier, A. Raybaud, R. Sauve, and L. Parent. 2004. Negatively charged residues in the N-terminal of the AID helix confer slow voltage dependent inactivation gating to CaV1.2. *Biophys. J.* 87:3181–3192.

Davies, A., J. Hendrich, A.T. Van Minh, J. Wratten, L. Douglas, and A.C. Dolphin. 2007. Functional biology of the alpha(2)delta subunits of voltage-gated calcium channels. *Trends Pharmacol. Sci.* 28:220–228.

De Waard, M., and K.P. Campbell. 1995. Subunit regulation of the neuronal alpha 1A Ca2+ channel expressed in Xenopus oocytes. *J. Physiol.* 485:619–634.

DeMaria, C.D., T.W. Soong, B.A. Alseikhan, R.S. Alvania, and D.T. Yue. 2001. Calmodulin bifurcates the local Ca2+ signal that modulates P/Q-type Ca2+ channels. *Nature.* 411:484–489.

Dick, I.E., M.R. Tadross, H. Liang, L.H. Tay, W. Yang, and D.T. Yue. 2008. A modular switch for spatial Ca2+ selectivity in the calmodulin regulation of CaV channels. *Nature.* 451:830–834.

Dolphin, A.C. 2003. Beta subunits of voltage-gated calcium channels. *J. Bioenerg. Biomembr.* 35:599–620.

Edelhoch, H. 1967. Spectroscopic determination of tryptophan and tyrosine in proteins. *Biochemistry.* 6:1948–1954.

Erickson, M.G., H. Liang, M.X. Mori, and D.T. Yue. 2003. FRET two-hybrid mapping reveals function and location of L-type Ca2+ channel CaM preassociation. *Neuron.* 39:97–107.

Fallon, J.L., D.B. Halling, S.L. Hamilton, and F.A. Quiocho. 2005. Structure of calmodulin bound to the hydrophobic IQ domain of the cardiac Ca(v)1.2 calcium channel. *Structure.* 13:1881–1886.

Ferreira, G., J. Yi, E. Rios, and R. Shirokov. 1997. Ion-dependent inactivation of barium current through L-type calcium channels. *J. Gen. Physiol.* 109:449–461.

Findlay, I. 2004. Physiological modulation of inactivation in L-type Ca2+ channels: one switch. *J. Physiol.* 554:275–283.

Geib, S., G. Sandoz, V. Cornet, K. Mabrouk, O. Fund-Saunier, D. Bichet, M. Villaz, T. Hoshi, J.M. Sabatier, and M. De Waard. 2002. The interaction between the I-II loop and the III-IV loop of Cav2.1 contributes to voltage-dependent inactivation in a beta -dependent manner. *J. Biol. Chem.* 277:10003–10013.

Geourjon, C., and G. Deleage. 1995. SOPMA: significant improvements in protein secondary structure prediction by consensus prediction from multiple alignments. *Comput. Appl. Biosci.* 11:681–684.

Goldin, A.L. 2003. Mechanisms of sodium channel inactivation. *Curr. Opin. Neurobiol.* 13:284–290.

Grueter, C.E., S.A. Abiria, I. Dzhura, Y. Wu, A.J. Ham, P.J. Mohler, M.E. Anderson, and R.J. Colbran. 2006. L-type Ca2+ channel facilitation mediated by phosphorylation of the beta subunit by CaMKII. *Mol. Cell.* 23:641–650.

Hadley, R.W., and W.J. Lederer. 1991. Ca2+ and voltage inactivate Ca2+ channels in guinea-pig ventricular myocytes through independent mechanisms. *J. Physiol.* 444:257–268.

Halling, D.B., P. Aracena-Parks, and S.L. Hamilton. 2006. Regulation of voltage-gated Ca2+ channels by calmodulin. *Sci. STKE.* 2006:er1.

Hanlon, M.R., N.S. Berrow, A.C. Dolphin, and B.A. Wallace. 1999. Modelling of a voltage-dependent Ca2+ channel beta subunit as a basis for understanding its functional properties. *FEBS Lett.* 445:366–370.

He, L.L., Y. Zhang, Y.H. Chen, Y. Yamada, and J. Yang. 2007. Functional modularity of the beta-subunit of voltage-gated Ca2+ channels. *Biophys. J.* 93:834–845.

Herlitze, S., G.H. Hockerman, T. Scheuer, and W.A. Catterall. 1997. Molecular determinants of inactivation and G protein modulation in the intracellular loop connecting domains I and II of the calcium channel alpha1A subunit. *Proc. Natl. Acad. Sci. USA.* 94:1512–1516.

Hille, B. 2001. Ion Channels of Excitable Membranes. 3rd edition. Sinauer Associates, Inc., Sunderland, MA. 814 pp.

Hudmon, A., H. Schulman, J. Kim, J.M. Maltez, R.W. Tsien, and G.S. Pitt. 2005. CaMKII tethers to L-type Ca2+ channels, establishing a local and dedicated integrator of Ca2+ signals for facilitation. *J. Cell Biol.* 171:537–547.

Ivanina, T., Y. Blumenstein, E. Shistik, R. Barzilai, and N. Dascal. 2000. Modulation of L-type Ca2+ channels by gbeta gamma and calmodulin via interactions with N and C termini of alpha 1C. *J. Biol. Chem.* 275:39846–39854.

Kanevsky, N., and N. Dascal. 2006. Regulation of maximal open probability is a separable function of $Ca_v\beta$ subunit in L-type Ca^{2+} channel, dependent on NH_2 terminus of α_{1C} ($Ca_v1.2\alpha$). *J. Gen. Physiol.* 128:15–36.

Kapust, R.B., J. Tozser, J.D. Fox, D.E. Anderson, S. Cherry, T.D. Copeland, and D.S. Waugh. 2001. Tobacco etch virus protease: mechanism of autolysis and rational design of stable mutants with wild-type catalytic proficiency. *Protein Eng.* 14:993–1000.

Kim, J., S. Ghosh, D.A. Nunziato, and G.S. Pitt. 2004. Identification of the components controlling inactivation of voltage-gated Ca2+ channels. *Neuron.* 41:745–754.

Kobrinsky, E., S. Tiwari, V.A. Maltsev, J.B. Harry, E. Lakatta, D.R. Abernethy, and N.M. Soldatov. 2005. Differential role of the alpha1C subunit tails in regulation of the Cav1.2 channel by membrane potential, beta subunits, and Ca2+ ions. *J. Biol. Chem.* 280:12474–12485.

Lee, K.S., E. Marban, and R.W. Tsien. 1985. Inactivation of calcium channels in mammalian heart cells: joint dependence on membrane potential and intracellular calcium. *J. Physiol.* 364:395–411.

Lee, T.S., R. Karl, S. Moosmang, P. Lenhardt, N. Klugbauer, F. Hofmann, T. Kleppisch, and A. Welling. 2006. Calmodulin kinase II is involved in voltage-dependent facilitation of the L-type Cav1.2 calcium channel: identification of the phosphorylation sites. *J. Biol. Chem.* 281:25560–25567.

Liang, H., C.D. DeMaria, M.G. Erickson, M.X. Mori, B.A. Alseikhan, and D.T. Yue. 2003. Unified mechanisms of Ca(2+) regulation across the Ca(2+) channel family. *Neuron.* 39:951–960.

Lifson, S., and A. Roig. 1961. On the theory of helix-coil transitions in polypeptides. *J. Chem. Phys.* 34:1963–1974.

Long, S.B., E.B. Campbell, and R. Mackinnon. 2005. Crystal structure of a mammalian voltage-dependent Shaker family K+ channel. *Science.* 309:897–903.

Marqusee, S., and R.L. Baldwin. 1987. Helix stabilization by Glu-...Lys+ salt bridges in short peptides of de novo design. *Proc. Natl. Acad. Sci. USA.* 84:8898–8902.

Neely, A., X. Wei, R. Olcese, L. Birnbaumer, and E. Stefani. 1993. Potentiation by the beta subunit of the ratio of the ionic current to the charge movement in the cardiac calcium channel. *Science.* 262:575–578.

O'Neil, K.T., and W.F. DeGrado. 1990. A thermodynamic scale for the helix-forming tendencies of the commonly occurring amino acids. *Science.* 250:646–651.

Olcese, R., N. Qin, T. Schneider, A. Neely, X. Wei, E. Stefani, and L. Birnbaumer. 1994. The amino terminus of a calcium channel

Downloaded from http://rupress.org/jgp/article-pdf/133/3/327/1914330/jgp_200810143.pdf by guest on 09 February 2026

beta subunit sets rates of channel inactivation independently of the subunit's effect on activation. *Neuron*. 13:1433–1438.

Opatowsky, Y., C.C. Chen, K.P. Campbell, and J.A. Hirsch. 2004. Structural analysis of the voltage-dependent calcium channel beta subunit functional core and its complex with the alpha1 interaction domain. *Neuron*. 42:387–399.

Patgiri, A., A.L. Jochim, and P.S. Arora. 2008. A hydrogen bond surrogate approach for stabilization of short peptide sequences in alpha-helical conformation. *Acc. Chem. Res.* 41:1289–1300.

Perez-Reyes, E., A. Castellano, H.S. Kim, P. Bertrand, E. Baggstrom, A.E. Lacerda, X.Y. Wei, and L. Birnbaumer. 1992. Cloning and expression of a cardiac/brain beta subunit of the L-type calcium channel. *J. Biol. Chem.* 267:1792–1797.

Pitt, G.S. 2007. Calmodulin and CaMKII as molecular switches for cardiac ion channels. *Cardiovasc. Res.* 73:641–647.

Qin, N., D. Platano, R. Olcese, J.L. Costantin, E. Stefani, and L. Birnbaumer. 1998. Unique regulatory properties of the type 2a Ca2+ channel beta subunit caused by palmitoylation. *Proc. Natl. Acad. Sci. USA*. 95:4690–4695.

Raybaud, A., Y. Dodier, P. Bissonnette, M. Simoes, D.G. Bichet, R. Sauve, and L. Parent. 2006. The role of the GX9GX3G motif in the gating of high voltage-activated Ca2+ channels. *J. Biol. Chem.* 281:39424–39436.

Raybaud, A., E.E. Baspinar, F. Dionne, Y. Dodier, R. Sauve, and L. Parent. 2007. The role of distal S6 hydrophobic residues in the voltage-dependent gating of CaV2.3 channels. *J. Biol. Chem.* 282:27944–27952.

Restituito, S., T. Cens, C. Barrere, S. Geib, S. Galas, M. De Waard, and P. Charnet. 2000. The [beta]2a subunit is a molecular groom for the Ca2+ channel inactivation gate. *J. Neurosci.* 20: 9046–9052.

Richard, S., E. Perrier, J. Fauconnier, R. Perrier, L. Pereira, A.M. Gomez, and J.P. Benitah. 2006. 'Ca(2+)-induced Ca(2+) entry' or how the L-type Ca(2+) channel remodels its own signalling pathway in cardiac cells. *Prog. Biophys. Mol. Biol.* 90:118–135.

Richards, M.W., J. Leroy, W.S. Pratt, and A.C. Dolphin. 2007. The HOOK-domain between the SH3 and the GK domains of CaVbeta subunits contains key determinants controlling calcium channel inactivation. *Channels*. 1:92–101.

Rohl, C.A., A. Chakrabartty, and R.L. Baldwin. 1996. Helix propagation and N-cap propensities of the amino acids measured in alanine-based peptides in 40 volume percent trifluoroethanol. *Protein Sci.* 5:2623–2637.

Shi, C., and N.M. Soldatov. 2002. Molecular determinants of voltage-dependent slow inactivation of the Ca2+ channel. *J. Biol. Chem.* 277:6813–6821.

Shiraki, K., K. Nishikawa, and Y. Goto. 1995. Trifluoroethanol-induced stabilization of the alpha-helical structure of beta-lactoglobulin: implication for non-hierarchical protein folding. *J. Mol. Biol.* 245:180–194.

Sokolov, S., R.G. Weiss, B. Kurka, F. Gapp, and S. Hering. 1999. Inactivation determinant in the I-II loop of the Ca2+ channel alpha1-subunit and beta-subunit interaction affect sensitivity for the phenylalkylamine (-)gallopamil. *J. Physiol.* 519:315–322.

Soldatov, N.M. 2003. Ca2+ channel moving tail: link between Ca2+-induced inactivation and Ca2+ signal transduction. *Trends Pharmacol. Sci.* 24:167–171.

Splawski, I., K.W. Timothy, L.M. Sharpe, N. Decher, P. Kumar, R. Bloise, C. Napolitano, P.J. Schwartz, R.M. Joseph, K. Condouris, et al. 2004. Ca(V)1.2 calcium channel dysfunction causes a multisystem disorder including arrhythmia and autism. *Cell.* 119:19–31.

Splawski, I., K.W. Timothy, N. Decher, P. Kumar, F.B. Sachse, A.H. Beggs, M.C. Sanguinetti, and M.T. Keating. 2005. Severe arrhythmia disorder caused by cardiac L-type calcium channel mutations. *Proc. Natl. Acad. Sci. USA*. 102:8089–8096.

Stea, A., W.J. Tomlinson, T.W. Soong, E. Bourinet, S.J. Dubel, S.R. Vincent, and T.P. Snutch. 1994. Localization and functional properties of a rat brain alpha 1A calcium channel reflect similarities to neuronal Q- and P-type channels. *Proc. Natl. Acad. Sci. USA*. 91:10576–10580.

Stotz, S.C., and G.W. Zamponi. 2001. Structural determinants of fast inactivation of high voltage-activated Ca(2+) channels. *Trends Neurosci.* 24:176–181.

Stotz, S.C., J. Hamid, R.L. Spaetgens, S.E. Jarvis, and G.W. Zamponi. 2000. Fast inactivation of voltage-dependent calcium channels. A hinged-lid mechanism? *J. Biol. Chem.* 275:24575–24582.

Stotz, S.C., S.E. Jarvis, and G.W. Zamponi. 2004. Functional roles of cytoplasmic loops and pore lining transmembrane helices in the voltage-dependent inactivation of HVA calcium channels. *J. Physiol.* 554:263–273.

Tadross, M.R., I.E. Dick, and D.T. Yue. 2008. Mechanism of local and global Ca2+ sensing by calmodulin in complex with a Ca2+ channel. *Cell.* 133:1228–1240.

Tareilus, E., M. Roux, N. Qin, R. Olcese, J. Zhou, E. Stefani, and L. Birnbaumer. 1997. A Xenopus oocyte beta subunit: evidence for a role in the assembly/expression of voltage-gated calcium channels that is separate from its role as a regulatory subunit. *Proc. Natl. Acad. Sci. USA*. 94:1703–1708.

Ulbricht, W. 2005. Sodium channel inactivation: molecular determinants and modulation. *Physiol. Rev.* 85:1271–1301.

Van Petegem, F., and D.L. Minor. 2006. The structural biology of voltage-gated calcium channel function and regulation. *Biochem. Soc. Trans.* 34:887–893.

Van Petegem, F., K.A. Clark, F.C. Chatelain, and D.L. Minor Jr. 2004. Structure of a complex between a voltage-gated calcium channel beta-subunit and an alpha-subunit domain. *Nature.* 429:671–675.

Van Petegem, F., F.C. Chatelain, and D.L. Minor Jr. 2005. Insights into voltage-gated calcium channel regulation from the structure of the CaV1.2 IQ domain-Ca2+/calmodulin complex. *Nat. Struct. Mol. Biol.* 12:1108–1115.

Van Petegem, F., K.E. Duderstadt, K.A. Clark, M. Wang, and D.L. Minor Jr. 2008. Alanine-scanning mutagenesis defines a conserved energetic hotspot in the Ca(V)alpha(1) AID-Ca(V)beta interaction site that is critical for channel modulation. *Structure.* 16:280–294.

Wang, D., K. Chen, J.L. Kulp, and P.S. Arora. 2006. Evaluation of biologically relevant short alpha-helices stabilized by main-chain hydrogen bond surrogate. *J. Am. Chem. Soc.* 128:9248–9256.

Yamaguchi, H., M. Okuda, G. Mikala, K. Fukasawa, and G. Varadi. 2000. Cloning of the beta(2a) subunit of the voltage-dependent calcium channel from human heart: cooperative effect of alpha(2)/delta and beta(2a) on the membrane expression of the alpha(1C) subunit. *Biochem. Biophys. Res. Commun.* 267:156–163.

Yasuda, T., L. Chen, W. Barr, J.E. McRory, R.J. Lewis, D.J. Adams, and G.W. Zamponi. 2004. Auxiliary subunit regulation of high-voltage activated calcium channels expressed in mammalian cells. *Eur. J. Neurosci.* 20:1–13.

Yuan, W., and D.M. Bers. 1994. Ca-dependent facilitation of cardiac Ca current is due to Ca-calmodulin-dependent protein kinase. *Am. J. Physiol.* 267:H982–H993.

Zhang, J.F., P.T. Ellinor, R.W. Aldrich, and R.W. Tsien. 1994. Molecular determinants of voltage-dependent inactivation in calcium channels. *Nature.* 372:97–100.

Zhang, R., I. Dzhura, C.E. Grueter, W. Thiel, R.J. Colbran, and M.E. Anderson. 2005. A dynamic alpha-beta inter-subunit agonist signaling complex is a novel feedback mechanism for regulating L-type Ca2+ channel opening. *FASEB J.* 19:1573–1575.

Downloaded from http://rupress.org/jgp/article-pdf/133/3/327/1914330/jgp_200810143.pdf by guest on 09 February 2026

Zimm, B.H., and J.K. Bragg. 1959. Theory of the phase transition between helix and random coil in polypeptide chains. *J. Chem. Phys.* 31:526–535.

Zühlke, R.D., and H. Reuter. 1998. Ca2+-sensitive inactivation of L-type Ca2+ channels depends on multiple cytoplasmic amino acid sequences of the alpha1C subunit. *Proc. Natl. Acad. Sci. USA.* 95:3287–3294.

Zühlke, R.D., G.S. Pitt, K. Deisseroth, R.W. Tsien, and H. Reuter. 1999. Calmodulin supports both inactivation and facilitation of L-type calcium channels. *Nature.* 399:159–162.

Zühlke, R.D., G.S. Pitt, R.W. Tsien, and H. Reuter. 2000. Ca2+-sensitive inactivation and facilitation of L-type Ca2+ channels both depend on specific amino acid residues in a consensus calmodulin-binding motif in the (alpha)1C subunit. *J. Biol. Chem.* 275:21121–21129.

Downloaded from http://rupress.org/jgp/article-pdf/133/3/327/1914330/jgp_200810143.pdf by guest on 09 February 2026